AD NUMBER

AD476380

NEW LIMITATION CHANGE

TO

Approved for public release, distribution unlimited

FROM

Distribution authorized to U.S. Gov't. agencies and their contractors; Critical Technology; NOV 1965. Other requests shall be referred to Air Force Weapons Laboratory, ATTN: WLRT, Kirtland AFB, NM 87117.

AUTHORITY

AFWL ltr dtd 30 Nov 1971

OPACITY OF LOW TEMPERATURE AIR

D. E. Buttrey
H. R. McChesney

Lockheed Missiles and Space Company
Physical Sciences Laboratory
Palo Alto, California

Contract AF29(601)-6433

TECHNICAL REPORT NO. AFWL-TR-65-134
November 1965

AIR FORCE WEAPONS LABORATORY
Research and Technology Division
Air Force Systems Command
Kirtland Air Force Base
New Mexico

Research and Technology Division
AIR FORCE WEAPONS LABORATORY
Air Force Systems Command
Kirtland Air Force Base
New Mexico

OPACITY OF LOW TEMPERATURE AIR

D. E. Buttrey
H. R. McChesney
Lockheed Missiles and Space Company
Physical Sciences Laboratory
Palo Alto, California

FOREWORD

This report was prepared by the Lockheed Missile and Space Company, 3251 Hanover Street, Palo Alto, California, under Contract AF 29(601)-6433. The work was performed under Program Element 7.60.06.01.5, Project 5710, Subtask 07.003, and was funded by the Defense Atomic Support Agency (DASA). Inclusive dates of research were 1 July 1964 to 1 July 1965. The report was submitted 10 October 1965 by the Air Force Weapons Laboratory Project Officer, 2Lt Fred J. Reule (WLRT).

The author would like to thank Drs. R. E. Meyerott and J. E. Evans for their interest and help throughout this research, Mr. Lee Hooker for his capable assistance in the operation of the shock tube and in the analysis of the experimental data, and Mrs. Marcie Cleveland for assistance in preparation of the manuscript.

This technical report has been reviewed and is approved.

Fred J. Reule

FRED J. REULE
2Lt, USAF
Project Officer

Ralph H. Pennington

RALPH H. PENNINGTON
Lt Colonel, USAF
Chief, Theoretical Branch

William H. Stephens

WILLIAM H. STEPHENS
Colonel, USAF
Chief, Research Division

ABSTRACT

Emission spectrograms with 0.2 Angstrom resolution have been recorded for shock-heated air, oxygen, nitrogen, and nitrous oxide for temperatures from 6,000 to 12,000 degrees Kelvin and densities from 0.1 to 3.3 normal. The beta and gamma band systems of nitrous oxide were not observed in these spectra, leading to the conclusion that Bethke's f-values are at least a factor of two too high. A SACHA peak-to-minimum fit to the experimental profile of singly ionized molecular nitrogen 3914 Angstrom band head was found for a Lorentz line width of 1.9 per centimeters for the condition of 9,500 degrees Kelvin and 0.15 normal density in pure nitrogen. An upper limit for the molecular oxygen-atomic oxygen collision cross section of less than or equal to 2×10^{-14} square centimeters has been obtained from analysis of oxygen Schumann-Runge emission lines for the condition of 8,400 degrees Kelvin and 0.3 normal density. Absolute intensity measurements of nitrogen continuum radiation in the molecular regime below 12,000 degrees Kelvin have failed to show the intensity predicted by Boldt's negatively charged atomic nitrogen photodetachment cross section. The addition of lithium oxide to shocks in oxygen has failed to show any real evidence of the negatively charged atomic oxygen photoelectric edge at 3,600 Angstroms. However, SACHA experimental analyses of the oxygen Schumann-Runge rotational lines at 3,400 Angstroms has yielded some quantitative evidence of the existence of an edge underlying the molecular oxygen rotational line.

CONTENTS

ILLUSTRATIONS

TABLES

LIST OF SYMBOLS

λ	Wavelength in Angstroms
ν	Wave number in cm^{-1}
T_5	Reflected shock temperature in degrees Kelvin
p_1	Downstream starting pressure in shock tube in mm of Hg
f-value	Value of electronic transition probability or oscillator strength
N	Number density in particles per cm^3
v	Particle velocity in cm sec^{-1}
α_c	Optical collision diameter in cm
$\alpha_{mol-mol}$ and $\alpha_{mol-atom}$	The collision diameters which a molecule presents to a molecule and to an atom, respectively, for collision
σ	Half the width at half maximum of rotational lines in cm^{-1}
k	Gas constant = 1.38 x 10 erg deg^{-1}
m_{atom}, m_{mol}	The mass in gm of an atom and a molecule, respectively
m_t	$m_{atom} + m_{mol}$
v', v''	Vibration quantum number of the upper and lower electronic states, respectively
J', J''	The rotational quantum number of the upper and lower electronic states, respectively
U_s^{-1}	Reciprocal incident shock velocity in μsec per foot
T_λ	Fractional transmission of a gas sample at wavelength λ
I_λ^0, I_λ	The incident and transmitted intensities, respectively, at wavelength λ in ergs sec^{-1} cm^{-3}
x	Pathlength in cm
μ_λ	The absorption coefficient per cm at wavelength λ

$B_\lambda(T_5)$ Black body brightness in ergs sec^{-1} cm^{-2} $(\Delta\lambda)^{-1}$ $ster^{-1}$ at reflected shock temperature T_5

$\epsilon^{\lambda}_{total}$ Measured total gaseous emissivity at wavelength λ due to all processes

$\bar{\epsilon}$ Average emissivity

N(PE) Subscript referring to the nitrogen photoelectric process

ff(+), ff(neutral) Subscripts referring to the free-free transitions of electrons in the field of the positive ion and of the neutral atom, respectively

N^-(PD) and O^-(PD) Subscripts referring to the photodetachment of the electron from the N^- and O^- atoms, respectively

Ne, N_{ion} Electron and ion number densities in cm^{-3}

Z Charge on the ion

Ry Rydberg constant

u $h\nu/kT$

$g(u,\gamma^2)$ Temperature-averaged Gaunt factor for electron in Coulomb field

e, m Charge and mass of the electron

1. INTRODUCTION

In recent years a great deal of effort has gone into the theoretical and experimental determination of the spectral absorption coefficient of heated air (Refs. 1-15). This is an important problem since the transport of radiation through the atmosphere, as well as the emission from heated samples of the atmosphere, depends primarily upon the absorption coefficient. It is also a very complicated and difficult problem because of the large number of processes and interactions that occur in a heated atmosphere. Radiation transport codes (Refs. 14, 15) are under development whose success will depend critically upon the availability of accurate and detailed values of the absorption coefficient of air. There has been a progressive improvement in the accuracy of both the measurements and the calculations such that it is now appropriate to carry out comparisons to reinforce the validity of each approach and/or to uncover omissions or undiscovered errors.

In the molecular regime below 15,000°K, the problems may be divided into two reasonably distinct areas: (a) the problem of line absorption by discrete transitions, and (b) the problem of continuum absorption by continuum processes. The problem of rotational line widths and shapes is a very difficult and important problem. Due to overlapping of lines and splitting of rotational levels it is not possible to examine experimentally the shape or to measure the intensity of an individual rotational line. It is not yet possible to theoretically compute molecular wave functions and parameters with anywhere near the accuracy of the atomic calculations. Therefore, in the case of molecular structure appeal must be made to experimental results and a semi-empirical theoretical formulation based on experimental results. Radiation from continuum processes has no strong identifiable features such as the discrete spectrum. The experimentalist can measure only the total spectral intensity from all continuum processes. In the case of heated nitrogen there is an appreciable continuum contribution to the opacity for the range of thermodynamic conditions for which the visible spectrum is covered by a blanket of rotational lines. In

order to separate the continuum contribution from the discrete the experimentalist must rely on the accuracy of air transport codes such as the SACHA Code (Spectral Absorption Coefficient for Heated Air) (Ref. 14) to compute the line contribution. The accuracy of the computed line intensity is dependent on that of the experimental transition probabilities used in the calculation. Three or possibly four continuum processes may contribute to the total continuum intensity including recombination, photodetachment and free-free energy transitions of the electron in the field of the positive ion and neutral atom. The relative contributions of these to the continuum intensity vary in a complicated way with temperature and density. Thus, the experimentalist must attempt to isolate or enhance one process by varying thermodynamic conditions or by addition of impurities. This has been the approach used in this work.

The work reported here is part of a continuing program to determine the basic radiative properties of high-temperature air species. The conventional shock tube provides a means to determine transition probabilities, rotational line shapes, and photoelectric and photodetachment cross sections for the conditions of temperature and plasma densities encountered in actual problems where radiative transfer is important. Optically thin pathlengths in the centers of the emission lines in the molecular band systems are achieved by working at higher temperatures where the emissivity is reduced by fall off in the density of the molecule due to dissociation. A distinct advantage in rotational line profile studies of working in the high-temperature, emission regime is that the half-widths of the collision-broadened rotational lines are several tenths of an Angstrom, and thus amenable to study with spectrographs such as the f/3.5 Meinel spectrograph (Ref. 16) having a medium-high wavelength resolution (0.2 Å) and sufficient light-gathering power to record the equilibrium spectral time history.

The LMSC SACHA code has been set up to compute the spectral absorption and emission coefficients of heated air over the frequency interval and temperature range where electronic transitions in diatomic molecules are important. With the aid of experimentally determined constants, the spectra of six band systems have been reconstructed theoretically. These

spectra and the corresponding line intensities have been preserved in the form of a magnetic tape atlas. The SACHA program can be used to compute the detailed rotational-line intensity envelope in selected frequency bandpasses for any specified temperature, density and pathlength in heated air. The code uses a Lorentz line shape with a variable half-width input. It has been used to compute the integrated or average absorption coefficient for a given frequency interval to within a constant input factor, the f-number for the specie. Since the f-number enters the absorption coefficient calculations of each band system as a constant factor, errors introduced into the absorption coefficient calculation by incorrect electronic oscillator strengths can be eliminated by simple scaling. By the same token it is relatively simple to check on the validity of the input f-numbers by comparison of the calculated spectral intensity with the experimentally determined quantities, i.e., either the integrated intensity from a photomultiplier measurement in a narrow wavelength bandpass or the detailed intensity envelope displayed in a high-resolution spectrogram for the shock-heated equilibrium gas sample. By the latter comparison it is possible to determine the half-width of the rotational lines by variation of half-width input into the calculation until a fit is found to the experimental intensity profile. Further it is possible to determine the intensity contribution of the continuum in two ways: by subtraction of the calculated line contribution from the measured line-plus-continuum intensity, and by a newly developed technique of normalizing the detailed experimental spectral intensity profile to the calculated rotational line intensity envelope. This report describes how these techniques have been applied to selected spectral reg for high temperature air and its main constituents to check the consistency of our knowledge of the oscillator strengths for both discrete and continuum transitions which are important in air opacity.

2. SUMMARY

In the low-temperature molecular emission regime for heated equilibrium air between 5000°K and 12,000°K at near normal density the discrete rotational-vibrational band spectra for each of six electronic transitions in diatomic molecules are expected to appear in a calculable sequence, to blanket specific broad spectral ranges, and then to fade in intensity due to dissociation of the specie as the temperature is increased. The magnitude of the spectral line intensity at a given wavelength for a given molecular specie can in theory be calculated to within the accuracy of a constant factor called the f-value, or the oscillator strength for the transition. The f-values are experimentally determined quantities based on measured absorption or emission of spectral radiation by shock-heated gas samples (Refs. 3, 4, 6, 7, and 8) or arc-heated gas samples (Refs. 9, 10, 11, and 12), or inferred from the measurements of the mean lifetime of the upper electronic state for the transition using a pulsed electric discharge source (Ref. 13). These experiments are complex and significant errors can creep into individual f-values reported. When one employs these various f-values in an opacity code such as the LMSC SACHA program to predict the combined spectral intensity envelopes in selected spectral regions for a range of thermodynamic conditions in heated air, agreement with the experimental data may not be found in the sequence of appearance and disappearance for the lines of the various band systems. The truth lies in the spectral data. If inconsistencies with the calculated spectral intensities are found then it becomes necessary to re-examine the f-values employed in the calculations for the individual band systems. It is necessary to compare for the absolute magnitude and the relative magnitude of the intensity of the lines of one band system with respect to those of another.

The work described in this report represents the first attempt to be made to apply such leverage to the air opacity problem in the molecular regime. It requires the combination of two ingredients which have only

lately become available for such survey work: the LMSC SACHA opacity code (Ref. 14) and the Meinel spectrograph (Ref. 16 and Sec. 3b) which has high wavelength resolution (0.2 Å) and the light gathering power (f/3.5) required to record the equilibrium shock spectra of these band systems (Refs. 4 and 5). We have also applied this leverage to the study of rotational line profiles (Sec. 5) and to the determination of the shape and magnitude of the spectral continuum intensity underlying the nitrogen band systems (Sec. 6), and to the shape and magnitude of the O^- continuum under the O_2(S-R) band systems (Sec. 7), the results of which are discussed in the following paragraphs.

The transition probabilities for the six molecular rotational-vibrational band systems of interest in the opacity of heated air have come under scrutiny in the comparisons of the detailed rotational line intensity envelopes observed in high-resolution, emission spectrograms of shock-heated O_2, N_2, air, and NO, with the spectral intensity calculated by the LMSC SACHA code using various experimental f-values found in the literature. Experimental measurements of the averaged line-plus-continuum intensity for shock-heated N_2 in the molecular regime for nine narrow wavelength bandpasses covering the wavelength range from 3371 Å to 6050 Å have yielded quantitative checks on the transition probabilities of the N_2 Second Positive and First Positive transitions and for the N_2^+ First Negative system. Failure to observe the NOβ and NOγ bands and the N_2 First Positive bands in the high resolution spectrograms as predicted by the SACHA calculations allows the placement of an upper limit on the oscillator strengths for these transitions. The results of these comparisons are shown in the last column of Table 1, in which are also listed the f-values used in the present SACHA code and the f-values used by Breene and Nardone (Ref. 15) in their opacity calculations. The references to the experimental work from which the f-values were taken are given in the parentheses to the right of each entry.

Table 1

f-VALUES FOR THE SIX MOLECULAR TRANSITIONS OF INTEREST IN AIR OPACITY

System	Transition	Breene-Nardone	Present SACHA f-Values	This Work f-Values
N_2^+ (1-)	$B^2\Sigma_u^+ - X^2\Sigma_g^+$	0.035 (13)	0.0348 (13,4)	0.035 (4)
N_2 (2+)	$C^3\Pi_u - B^3\Pi_g$	0.038 (13)	0.07 (1)	0.040
N_2 (1+)	$B^3\Pi_g - A^3\Sigma_u^+$	0.025 (7)	0.02 (1)	0.003
O_2 (S-R)	$B^3\Sigma_u^- - X^3\Sigma_g^-$	0.163 (10)	0.048 (6)	0.048
NOβ	$B^2\Pi_u - X^2\Pi_g$	0.0015 (9)	0.008 (8)	≤0.0008
NOγ	$A^2\Sigma_u^+ - X^2\Pi_g$	0.0024 (9)	0.0025 (8)	≤0.0013

The f-value of 0.0348 for the N_2^+(1-) transition inferred from the Bennett Dalby measurements of the mean lifetime for the excited state (Ref. 13) and used in both the SACHA and the Breene and Nardone calculations has been confirmed by the work reported as well as by an extensive set of shock tube studies reported previously by Buttrey and Gibson (Ref. 4). The only check we have made on the Treanor-Wurster f-value of 0.048 for the O_2(S-R) systems in this work is by comparison of O_2(S-R) line intensity with the N_2(2+) line intensity. The Treanor-Wurster f-value of 0.048 has been used in detailed SACHA calculations of the spectral intensity envelopes for O_2 and for air reported here and, in general, the spectral intensity magnitudes predicted by its use do not seem amiss. In the intensity comparison arguments of the appearance with thermodynamic condition of one radiating specie versus others in the recorded spectra for air, a norm has to be chosen and the O_2(S-R) system with the Treanor-Wurster f-value of 0.048 is as good a choice as any.

A powerful technique has been developed for the determination of rotational line shapes and widths in the high-temperature molecular emission regime which promises to overcome to a large degree the problems of splitting of the rotational levels and overlapping of line profiles. Calculations

of the detailed intensity profile for selected clumps of rotational lines using the SACHA code with a variable line width input to a Lorentz shape are made for a range of half-widths until a fit to the high-resolution experimental shape is found for a given thermodynamic condition. The fitting of the calculated envelope is made on both a half-width basis and a peak-to-minimum intensity argument. A remarkable fit of the calculated with the experimental intensity envelope was found for the N_2^+ First Negative 3914 Å (0,0) band head region for the condition in shock-heated nitrogen of 9500°K and 0.125 ρ_o for the Lorentz line width of 1.9 cm^{-1}. Concentrations for this condition were N_2^+, 1.81 x 10^{15}; N_2, 6.2 x 10^{17}; N, 6.9 x 10^{18}; and N^+ and e, 3.45 x 10^{16} particles per cm^3. A similar analysis of the O_2 Schumann-Runge (0,14) line grouping at 3400 Å yielded a line width of 6 cm^{-1} for the condition of 8500°K and 0.33 ρ_o, which line width gave an O_2 - O optical collision cross section of $\leq 2 \times 10^{-14}$ cm^2. This value of the cross section is subject to change in the future when discrepancies in the rotational line frequency positions are cleared up in the SACHA calculations. This preliminary value is in basic agreement, however, with previous values of 0.78×10^{-14} cm^2 obtained by Treanor-Wurster, (Ref. 6) and of $\leq 10^{-14}$ cm^2 obtained by Krindach-Sobelev-Tunitski (Ref. 17).

Absolute intensity measurements of the line-plus-continuum radiation in shock-heated nitrogen below 12,000°K and at 0.124 ρ_o show that Boldt's N^- photodetachment cross sections (Ref. 12) of $\approx 10^{-16}$ cm^2 are many times too large, if indeed this negative ion is formed at all in the excited state. Neglecting N^- and assuming Karzas and Latter's cross sections (Ref. 18) for the free-free radiation of the electron in the field of the positive ion, the analysis of our data for 10,500°K yields nitrogen recombination cross sections varying from 6.2×10^{-22} cm^2 to 2.6×10^{-22} cm^2 between 2 eV and 4 eV.

Attempts to enhance and to observe the photoelectric edge of the O^- continuum at 3600 Å by the addition of small amounts of Li_2O into shock waves in oxygen are inconclusive. The expected change in the slope

of the background continuum intensity under the O_2 Schumann-Runge emission spectrum as compared to that observed for shocks in pure oxygen did not occur. However, some evidence of the existence of an edge in this wavelength region resulted from the experimental-SACHA study of the O_2 Schumann-Runge rotational lines at 3400 Å combined with absolute intensity measurements of line-plus-continuum radiation for shocks in pure oxygen. Our measured intensities for shock-heated O_2 at 8400°K and 0.33 ρ_o are in basic agreement with the O^- continuum intensities predicted by Branscomb's O^- photodetachment cross sections and the equilibrium concentration of O^- from shock calculations using Branscomb's value of 1.46 eV for the electron affinity of atomic oxygen.

3. INSTRUMENTATION

a. Shock Tube

The shock tube used in these experiments is a conventional shock tube made of stainless steel with a 3-inch inside diameter. Figure 1 is a schematic diagram of the shock tube arrangement. The driver section is 10 feet long and is equipped with Auburn SL spark plugs and choke coils to ignite the combustible gas mixture. The gas mixture that was used was 10 percent O_2, 20 percent H_2, and 70 percent He measured in terms of pressure, with total pressures before ignition between 300 and 400 psi. Stainless steel diaphragms were scribed with plus marks (+) of sufficient depth to allow the diaphragms to break when the pressure reached 1800 to 2000 psi after ignition. Barium titanate crystals were used as pressure sensors to measure the time per foot for passage of the incident shock front and scope-counter techniques were used for recording. Quartz windows were flush-mounted in the sides of the shock tube at the reflecting wall for viewing the radiation from the reflected shock. The reflecting wall was 23 feet from the diaphragm. The radiation from a thin rectangular slab of gas parallel to, and 3-5 mm from, the reflecting wall was viewed with three different spectrographs. The path length in the gas was 7.3 cm defined by the inside diameter of the shock tube.

To clean the shock tube a honing procedure was used to remove the copper and copper oxides deposited on the inside wall of the shock tube from previous usage of copper diaphragms and combustion driving. Acetone swabs were used for final cleaning. The silicone grease was used sparingly on the O-ring seals at each tube joint and at each window. Following each shot the combustion products were immediately removed, the tube was cleaned with the acetone swabs, and the quartz windows in the test section were replaced with new ones. Liquid nitrogen cold traps or acetone-and-dry ice traps were used on the vacuum forepump and diffusion pump and also on the mercury manometer. Before use of the rigorous cleaning procedure, the CN Violet bands were seen for shots in pure nitrogen along with many other unidentified impurity lines.

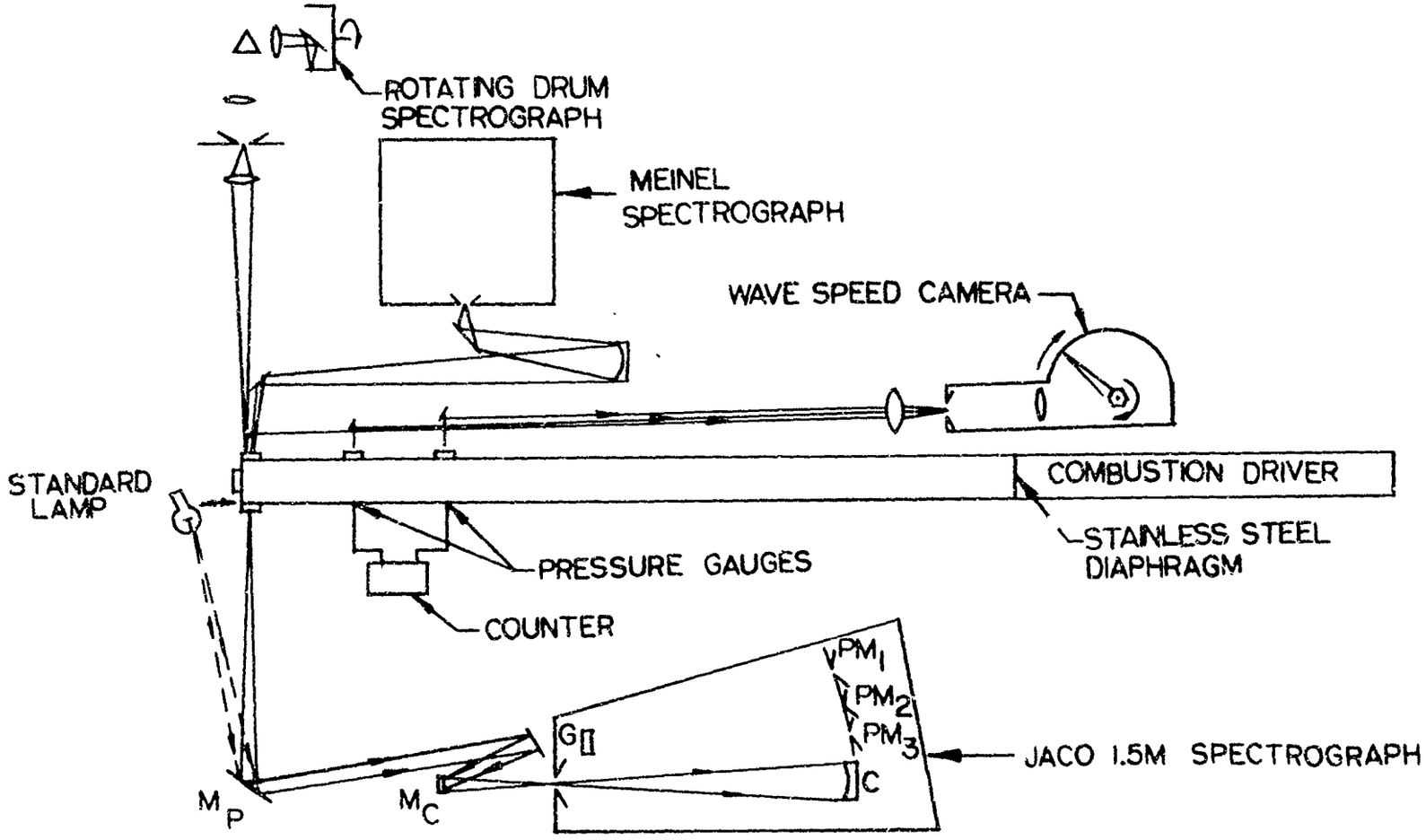

Fig. 1 Schematic Diagram of Shock Tube Instrumentation

b. Meinel Spectrograph

The Meinel Grating Spectrograph, shown in Fig. 2 (Ref. 16), was used to record reflected shock spectra with high wavelength resolution to get rotational line profiles. This spectrograph is unique in that it combines an effective geometrical aperture of f/3.5 with medium-high wavelength resolution of 0.2 Å in the second-order spectrum. The important optical component in this all-mirror instrument is a Schmidt corrector mirror, which corrects for the aberrations of the collimator mirror as well as those of the 21-inch camera mirror. Time resolution was achieved by a fast mechanical shutter that was placed at the entrance slit. It was triggered by the first radiation from the reflected shock by means of a photomultiplier placed inside the spectrograph. The shutter closed before the onset of nonequilibrium conditions in the field of view, allowing a spectral exposure time of 20 ± 5 μsec.

c. JACO 1.5-Meter Quantometer

Absolute intensity measurements were made with a JACO 1.5 meter grating spectrograph, Fig. 3, modified for use as a multi-channel quantometer by placing slits in the spectral focal plane. Radiation from selected wavelength bandpasses was received by photomultipliers mounted behind the focal plane. The output voltages of the photomultipliers were recorded on oscilloscopes which were triggered by one of the pressure gages. The voltage outputs from the photomultipliers were converted to absolute intensity units by comparison with the voltages recorded when a tungsten ribbon filament lamp of measured brightness temperature and known spectral emissivity was put effectively in the position of the shock tube side window. The radiation from the shock-heated gas was reduced by placing a rhodium neutral density filter at the entrance slit of the spectrograph. This was done to avoid non-linearity effects, i.e., to make the voltage outputs from the heated gas comparable in magnitude to relatively low voltage signals recorded for the standard lamp in the absence of the filter. RCA IP28 and RCA IP21 photomultipliers were used to record the radiation from the wavelength bandpasses at the spectral plane of the JACO Quantometer. A regulated dc power supply (John Fluke Model 402) was used to supply the voltage to each dynode. A

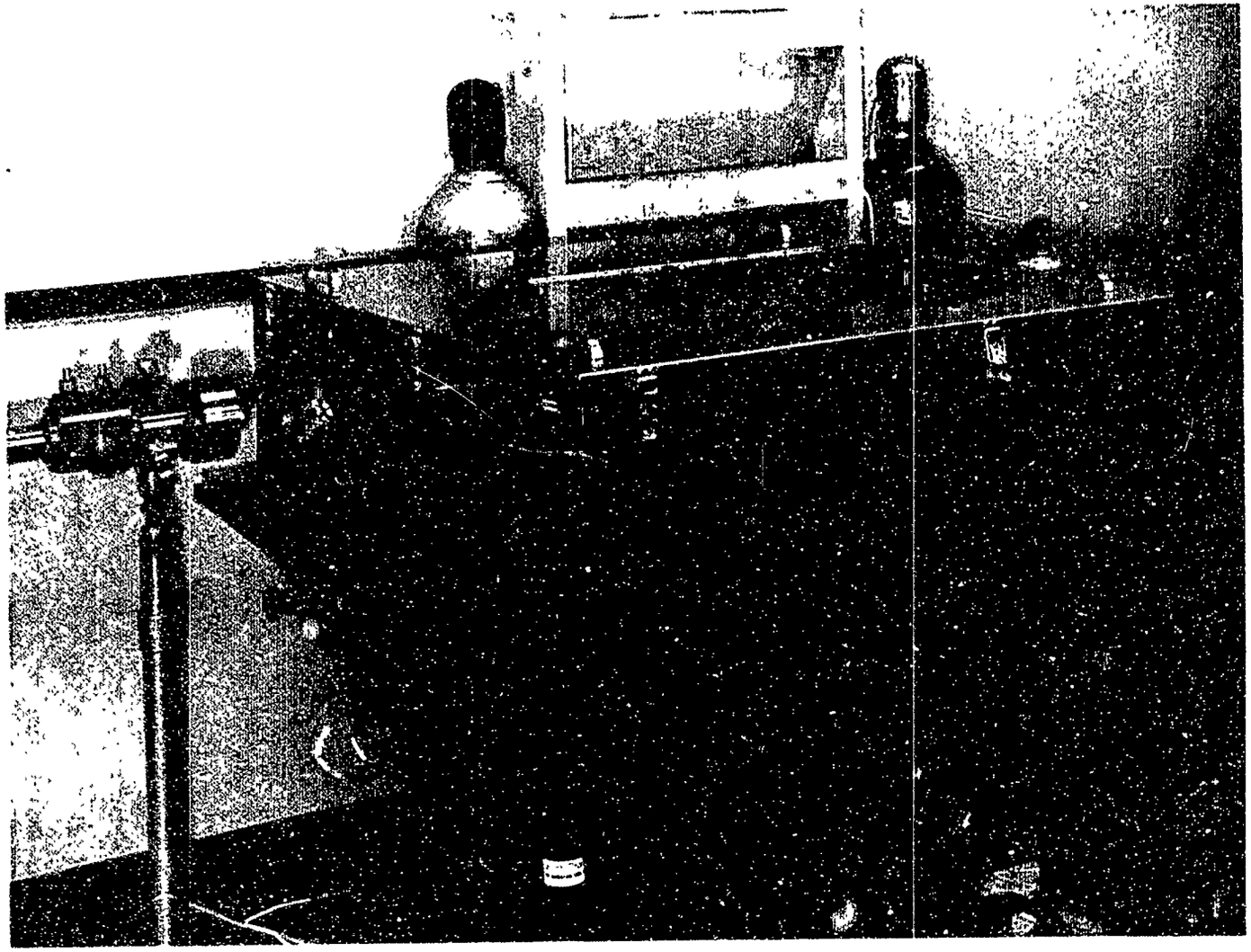

Fig. 2 Meinel Grating Spectrograph

Fig. 3 JACO 1.5 Meter Quantometer

differential voltmeter was used to measure the voltage to an accuracy of less than one volt in 1200 volts prior to each shot and prior to each intensity calibration with the standard lamp. Capacitors were placed across each stage to insure linearity in current drawn for as long as 200 μsec. A 10-kohm load resistor was used between the last dynode and ground. The voltage across this resistor was measured with Tektronix oscilloscopes. The effective RC time constant of the combination as used allowed a time resolution of less than 0.1 μsec. All voltages recorded were maintained less than 5 volts across the load resistor in order to prevent saturation effects.

Table 2 lists the wavelengths of the photomultiplier bandpasses used to make the absolute line-plus-continuum intensity measurements in the nitrogen continuum studies, Section 6. The 70 μ slit size used on the JACO 1.5-m Quantometer allowed a 0.1 Å resolution at the spectral focal plane; thus no slit function correction had to be applied to the measured intensities due to wavelength "smearing" across the bandpass. The positioning of the slits in the focal plane was achieved with much better precision than the wavelength spacing between rotational lines of ± 0.58 Å, as evidenced by spectrograms of the N_2 Geissler tube taken with the slits in position.

Table 2

WAVELENGTHS OF PHOTOMULTIPLIER BANDPASSES

N_2 CONTINUUM MEASUREMENTS

λ(Å)	Δλ(Å)
3362.4 - 3375.9	13.50
3414.7 - 3428.1	13.40
3898.8 - 3922.2	23.40
4005.8 - 4016.9	11.10
4710.5 - 4721.8	11.30
4997.0 - 5017.0	20.00
5309.4 - 5323.3	13.90
5655.0 - 5675.0	20.00
6069.0 - 6097.0	28.00

d. Gaertner Time-Resolved Spectrograph

A low-resolution streak spectrograph was made by combining a Gaertner constant-deviation, glass-prism spectrograph, Serial No. 205AW, with a Beckman Whitley drum camera, Model 224, as shown in Fig. 4. This combination had an effective aperture of f/10, which was sufficient to record the rotational-vibrational band systems of interest with 2 μsec time of exposure of I-F and I-N emulsions. The 2 μsec time resolution was achieved in the spectral time history of the reflected shock. Time resolution in streaked spectra is defined as the time required for the film to move the height of the slit image at the emulsion. The maximum speed of the film was 1/8 mm per μsec, which allowed for a total, continuous time coverage of 10^{-2} sec. The whole wavelength range accessible with glass optics could be covered with three different settings of the wavelength drum of the spectrograph. This instrument was found to be extremely useful in monitoring the time history of the Stark-broadened hydrogen lines (Refs. 3, 4) and in the determination of relative intensity with wavelength between 3900 Å and 7000 Å. The intensity of radiation from the incident shock was not high enough to be recorded by this spectrograph.

Fig. 4 Gaertner Time-Resolved Spectrograph

4. EMMISSION STUDIES OF THE NOβ AND NOγ SYSTEMS

a. Spectroscopic Background

NO is expected to be produced and to radiate in heated air in the temperature range 6000°K to 9000°K and between 10 and 10^{-3} normal density. The NOβ system, $B^2\Pi$ to $X^2\Pi_g$, 5200 Å to 2000 Å, and the NOγ system, $A^2\Sigma^+$ to $X^2\Pi_g$, 3000 Å to 2000 Å, are included as important radiators in the SACHA code (Ref. 14) and other air opacity tables (Refs. 1, 15). However, neither band system has been recorded in an identifiable way experimentally in either emission or absorption by heated air samples. Keck, et al. (Ref. 7) obtained the experimental f-values of 0.006 and 0.0025 for the NOβ and NOγ systems, respectively, by subtracting computed intensities of other radiating air species from the total measured spectral intensities in selected wavelength bandpasses and assigning the remaining intensity to NOβ and NOγ. The validity of this technique is doubtful. The voltage signal across the load resistor of a photomultiplier can have a limited value unless positive identification of the band systems contributing to that signal is made for recorded spectrograms for the equilibrium gas sample. Bethke (Ref. 9) obtained the f-values of 0.0015 and 0.0022 for the NOβ and γ systems, respectively. Meyerott, et al. (Ref. 1) and Churchill, et al. (Ref. 14) used the NOβ and γ f-values of 0.008 and 0.0025, respectively.

In order to resolve the questions surrounding these molecular band systems of NO the LMSC SACHA code has been used to calculate the detailed spectral emissivity for the 7.3 cm pathlength available in the shock-tube emission studies (Sec. 4b). The NO systems are expected to dominate the emission spectra (5000 Å to 2000 Å) of heated air for the thermodynamic conditions of 5000°K to 8000°K and normal density (Refs. 1 and 15). The NO systems are expected to be superimposed on the O_2 Schumann-Runge emission spectrum in the range from 5000°K to 7000°K and above 7000°K on the N_2 Second Positive spectrum. Since it has been possible to record the emission spectra of the O_2(S-R) systems and of the N_2(2+) systems in high resolution spectrograms of reflected shocks in pure oxygen and in pure nitrogen, respectively (Refs. 4 and 5), it is reasonable to expect to observe additional lines attributable to NOβ and γ systems for shocks in air and in shocks in NO if indeed any of these f-values is valid.

b. SACHA Calculations, NO Study

(1) Air at 6450°K and 0.74 ρ_o

The f-values of 0.0080 and 0.0025 for the NOβ and γ systems are presently being used in the LMSC SACHA code. Figure 5 shows the SACHA calculation using these f-values of the detailed spectral emissivity for a 7.3 cm pathlength for the condition of 6450°K and 0.74 normal density in heated air for which experimental data have been obtained. The frequency ranges of 29,550 cm^{-1} to 29,770 cm^{-1} and 3384 Å to 3360 Å were selected because the NOβ and γ lines which blanket the spectral range in a similar manner to the O_2(S-R) lines, i.e., do not "head-up" for easy identification, can be compared with the well-known, characteristic structure of the N_2(2+) 3371 Å (0,0) band (29,665 cm^{-1} to higher frequencies) expected to be relatively weak for this condition. Among several other v',v" transitions of the O_2(S-R) systems the strong 3370 Å (0,14) system (29,674 cm^{-1} to lower frequencies) is expected to contribute in this frequency range. The middle curve shows the SACHA calculation for the separate NO contribution to the spectral emissivity for this condition which ranges in general from 0.025 to 0.09 in this bandpass. The top curve is a calculation for the combined contributions of the O_2(S-R) and the NO (β, γ) systems for which the total emissivity ranges from 0.035 to 0.12. The important thing to notice is that the general structure of the O_2 - NO emission is dominated by the NO structure (middle curve) when the f-values of 0.0080 and 0.0025 are used for the NOβ and γ systems respectively. The same is true for the lower curve which adds the N_2(2+) systems to the O_2 - NO systems. The strong N_2(2+) 3371 Å (0,0) band head at 29,665 cm^{-1} does not show above the NO structure in the lower curve, even though a slight increase in the emissivity over that for the O_2 - NO (upper curve) is to be noted for the frequency range 29,665 cm^{-1} to 29770 cm^{-1}. In all of these calculations a Lorentz profile with a total width at half maximum of $2\sigma = 6$ cm^{-1} was used.

Figure 6 shows similar SACHA calculations for the same frequency region using Bethke's f-values of 0.0015 and 0.0022 for the NOβ and γ systems for the same heated-air condition of 6450°K and 0.74 normal density. The top

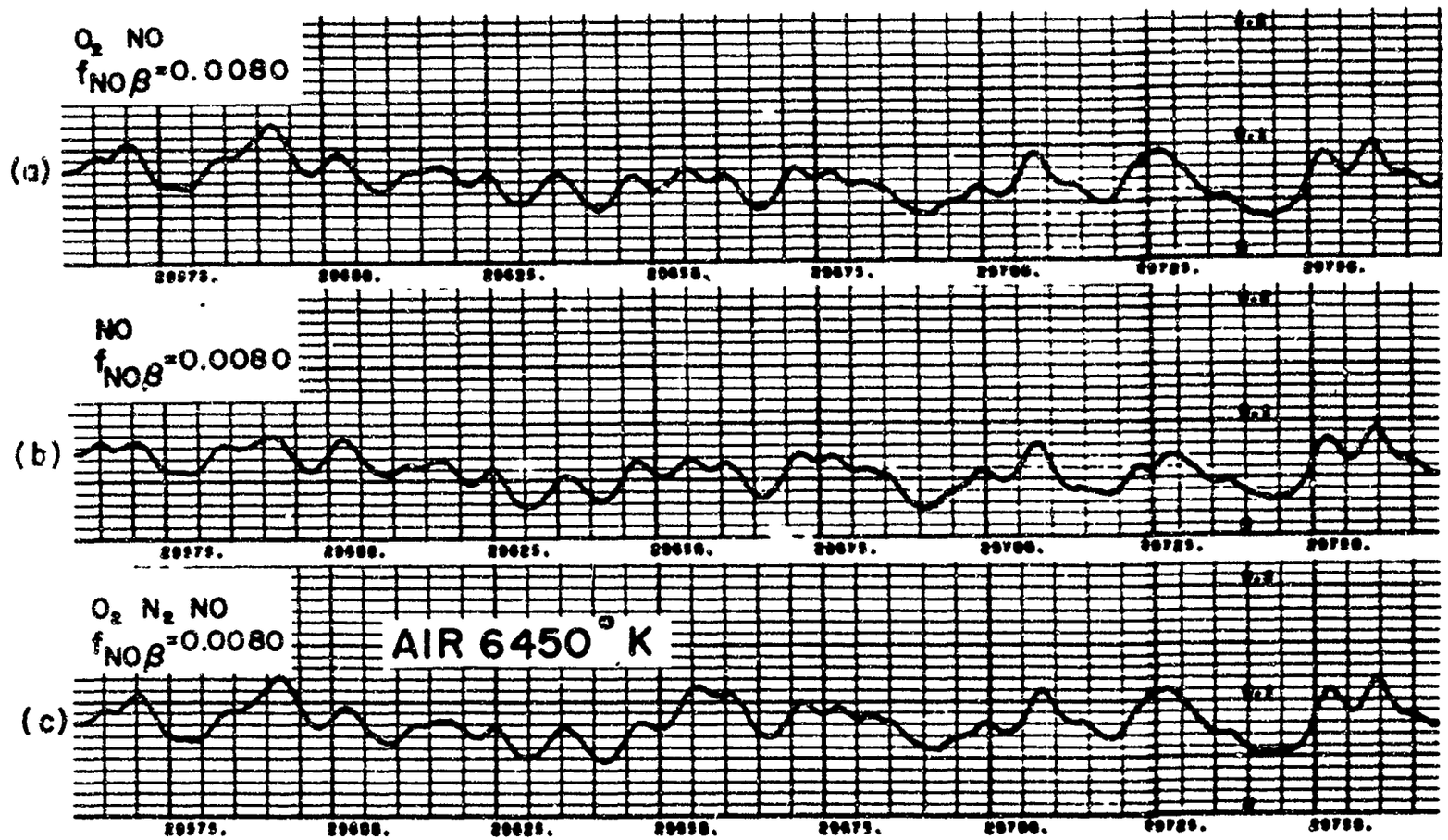

Fig. 5 SACHA Calculations of Detailed Spectral Emissivity for Air at 6450°K and 0.74 ρ_o Using the NOβ f-Value of 0.008

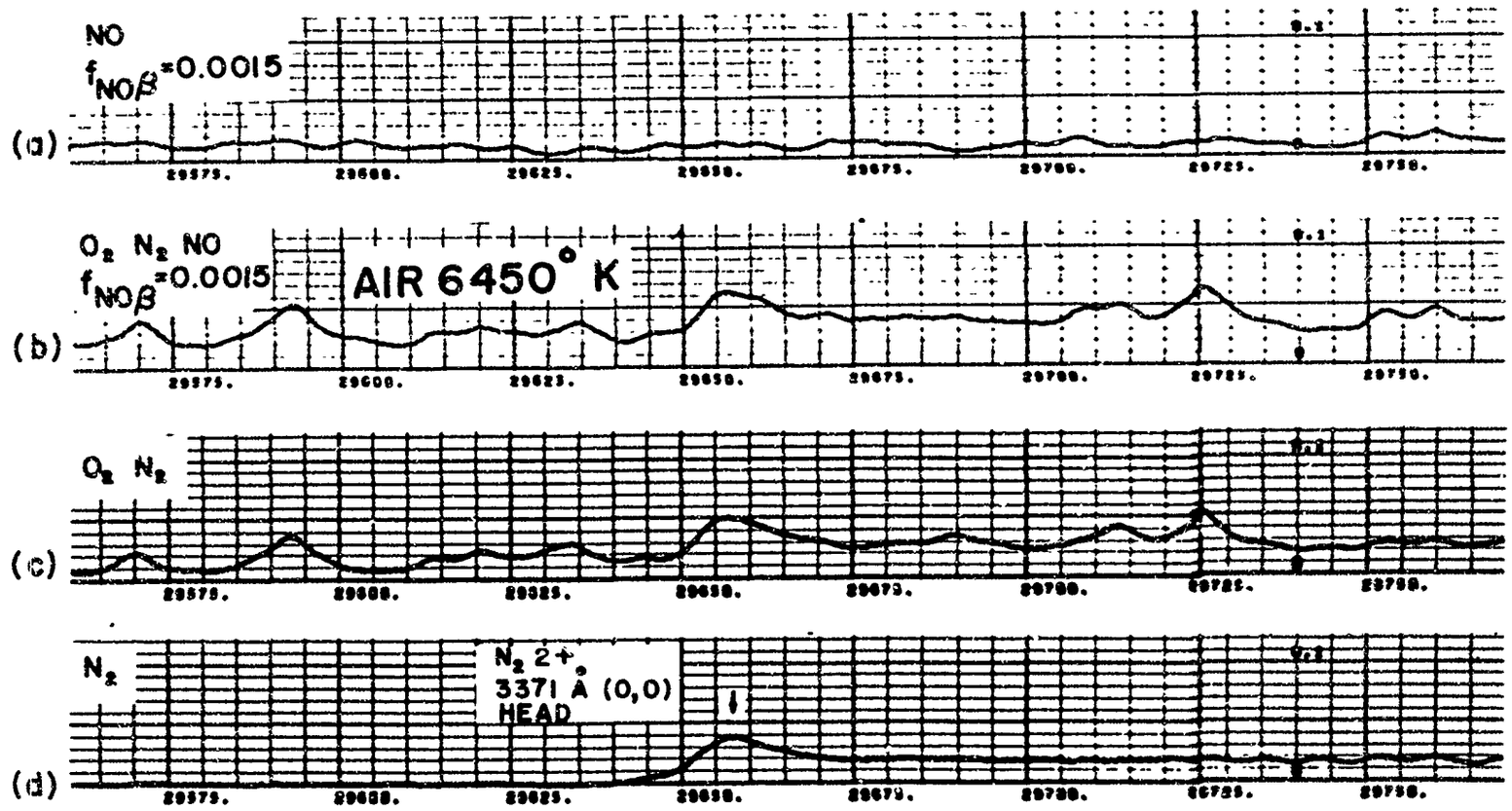

Fig. 6 SACHA Calculations of Detailed Spectral Emissivity for Air at 6450°K and 0.74 ρ_o Using the NOβ f-Value of 0.0015

curve (a) is for the emissivity contribution for NO which is essentially the middle curve of Fig. 5(b) reduced by a factor of one-fifth, i.e., the ratio of the NO(β) f-value of Bethke to that of 0.008. Curve (b) Fig. 6, is for the combined O_2 - N_2 - NO contributions, curve (c) is for the O_2 - N_2 contributions, and curve (d) is for the N_2 contribution only. Comparison of these four curves shows that the O_2(S-R) system should dominate the detailed structure of the spectral emissivity for frequencies in this range below 29,665 cm^{-1} and above this frequency the orderly structure of the $N_2(2+)(0,0)$ system, curve (d), is disturbed by the O_2 S-R system, curve (c). Detailed examination of the structure in curve (b) for the air mixture, i.e., the additive combination of curves (a) for NO and (c) for O_2 and N_2, shows some influence attributable to NO. This influence of NO structure can be considerably enhanced by plotting the emissivity on a log scale similar to that displayed in a densitometer trace of an experimental spectrogram.

It can be generally concluded from the SACHA calculations in Figs. 5 and 6 that the NOβ structure should dominate the spectral emissivity of air at 6450°K and 0.74 normal density if the NO f-value of 0.008 is correct, Fig. 5, and that the NO structure should be an observable in high resolution spectrograms if the NOβ and γ f-values are as high as those of Bethke, Fig. 6.

(2) Air at 7620°K and 0.85 ρ_o

For the condition of 7620°K and 0.85 ρ_o in heated air the $N_2(2+)$ systems are expected to be considerably stronger in intensity than shown for the 6450°K condition just discussed, and the O_2 S-R system are expected to have reduced intensity due to dissociation of the specie. Figure 7 shows SACHA calculations of spectral emissivity for the air mixture curve and for the contribution to that curve made by NO (mostly NOβ) using an f-value of 0.008 for the NOβ system in both calculations. The NO structure can be seen to dominate the structure to the left of the strong $N_2(2+)(0,0)$ band head and to influence the orderly structure of this $N_2(2+)$band system to the right (higher frequencies) of the $N_2(2+)$ band head.

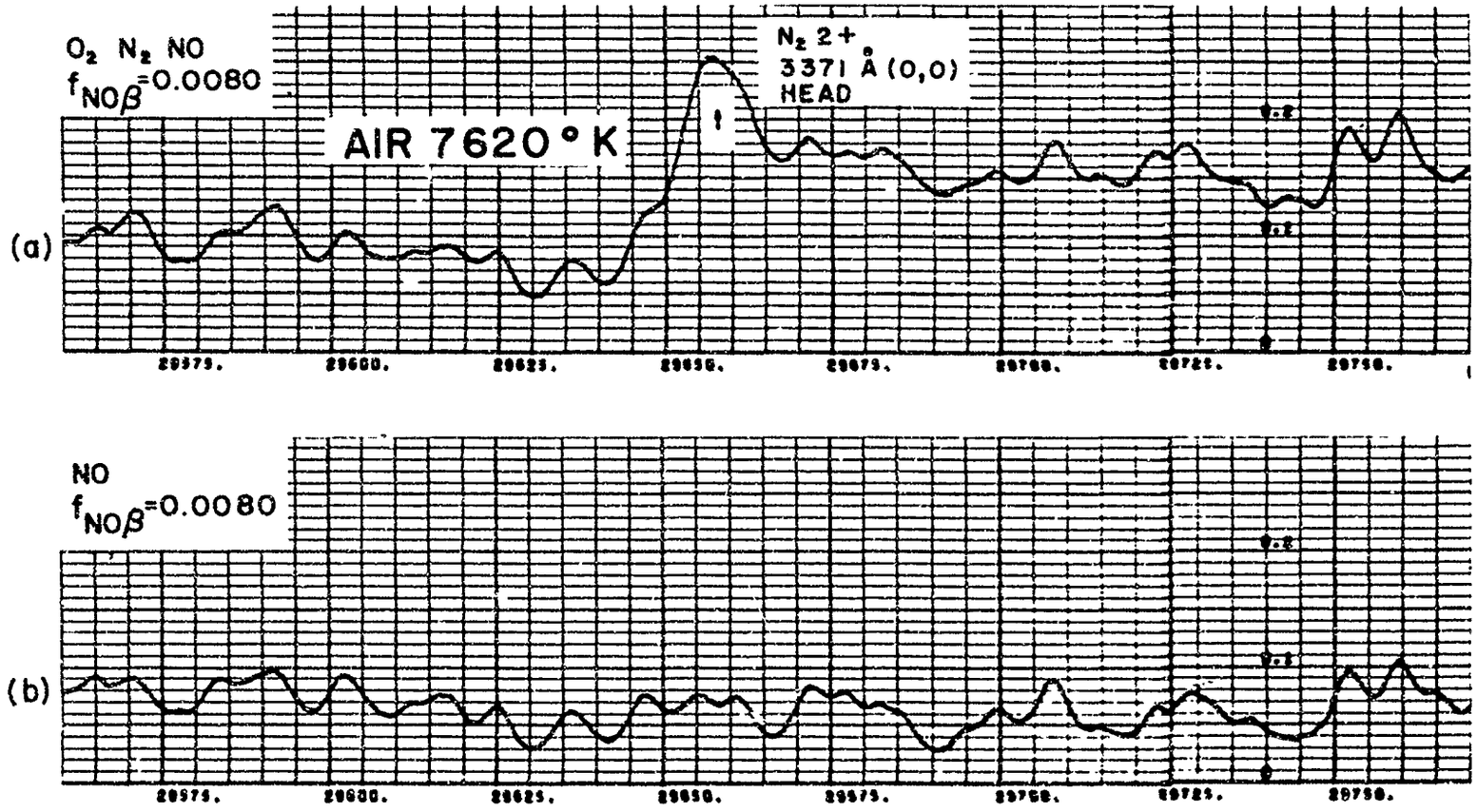

Fig. 7 SACHA Calculations of Detailed Spectral Emissivity for Air at 7620°K and 0.85 ρ_o Using the NOβ f-Value of 0.008

Figure 8 shows similar SACHA calculations of spectral emissivity for the air at 7620°K and 0.85 ρ_o, curve (c), and its contributing components, curve (a), (b), and (d) using Bethke's f-values. The NO emissivity contribution, curve (d), in this case is about one-third to one-half the total shown in the spectral region to the left of the strong $N_2(2+)$ 3371 Å (0,0) band. Therefore, the NO-line contribution should be observable in this spectral region in the high-resolution air spectrogram for this condition if the NO f-values are in fact as great as Bethke's values. The O_2 S-R lines should be observable though weak as seen in the comparison of the N_2 emissivity curve (a) with the O_2 - N_2 emissivity curve (b).

c. Experimental SACHA-Comparisons, NO Study

(1) Meinel Spectrograms for Shock-Heated O_2, Air, and N_2

Figure 9 shows portions of second-order Meinel spectrograms for shock heated O_2, air and N_2 in two sections covering the spectral range from 3577 Å to 2640 Å. The low-temperature N_2 Geissler tube electric discharge spectrum is included as a wavelength standard showing the second-order $N_2(2+)$ spectrum, top, and the first-order $N_2(1+)$ spectrum on the very bottom. The spectrum for O_2 at 6250°K and ρ_o is the O_2 Schumann-Runge emission spectrum below which is the remarkably similar spectrogram for equilibrium air at 6450°K and 0.74 ρ_o. The next spectrum below is for air at 7620°K and 0.85 ρ_o which is to be compared with $N_2(2+)$ spectrum for N_2 at 9500°K and 0.124 ρ_o. These two spectra were recorded on Eastman-Kodak 1-F emulsion which is sensitive up to 6700 Å and, since no filters were used to sort the first and second orders, the $N_2(1+)$ systems identified in the N_2 STD (very bottom) should be visible, if important, superimposed on the second order $N_2(2+)$ spectrum below 3300 Å. This should be true for both the N_2 (9500°K) and the 7620°K air spectra. The only weak indication of $N_2(1+)$ system is for the first-order wavelength 6788 Å indicated by two dots (..). Thus, these spectra show that the $N_2(1+)$ system, as well as the NO β and γ systems, are relatively unimportant radiators for these thermodynamic conditions, as compared to the $N_2^+(1-)$ (not shown in this wavelength range), the $N_2(2+)$, and the O_2(S-R) systems. Selected portions of spectra such as these for air, pure O_2 and pure N_2 have been chosen for detailed comparisons of rotational-line intensity envelopes in an effort to resolve the questions surrounding

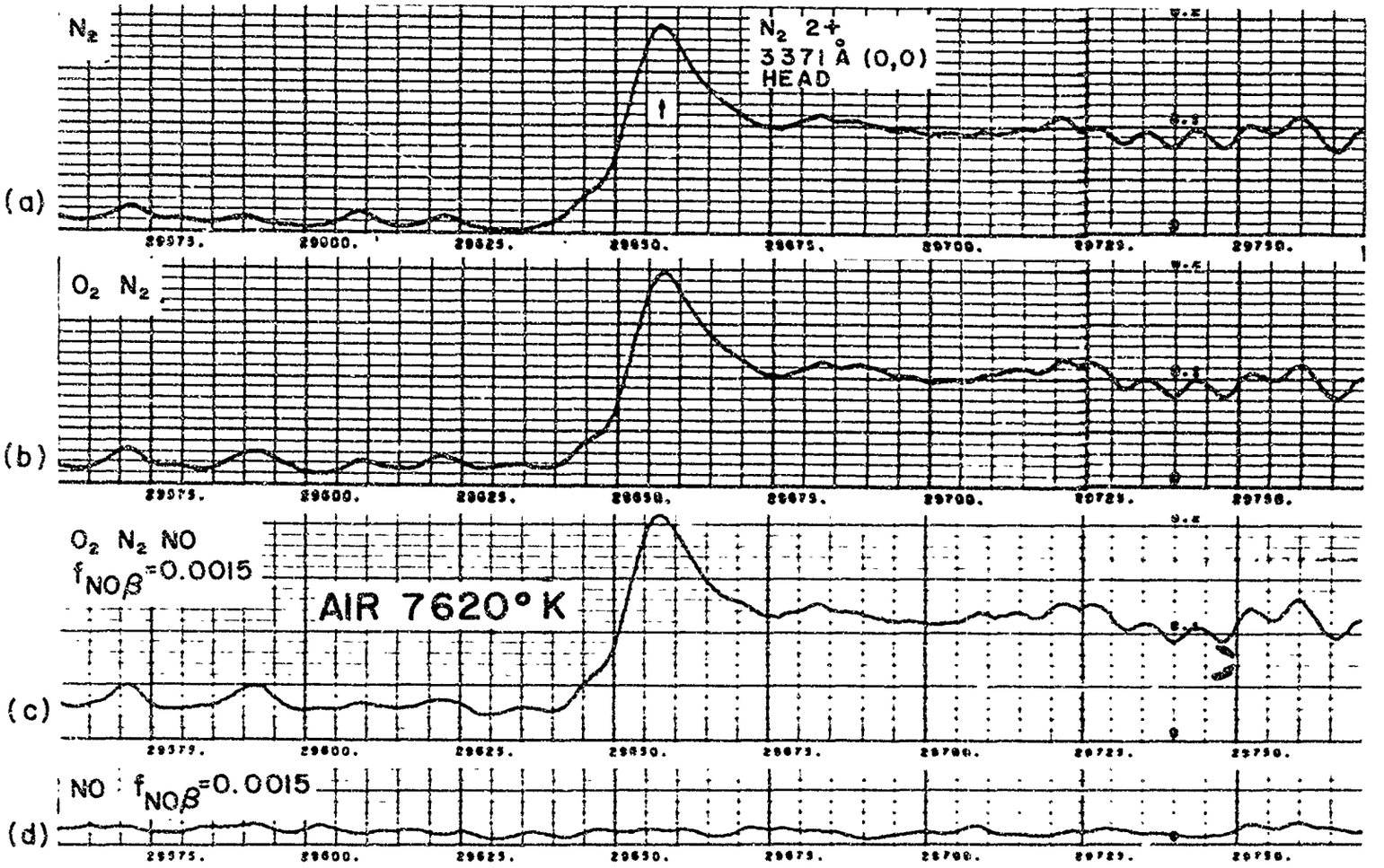

Fig. 8 SACHA Calculations of Detailed Spectral Emissivity for Air at 7620°K and 0.85 ρ_o Using the NOβ f-Value of 0.0015

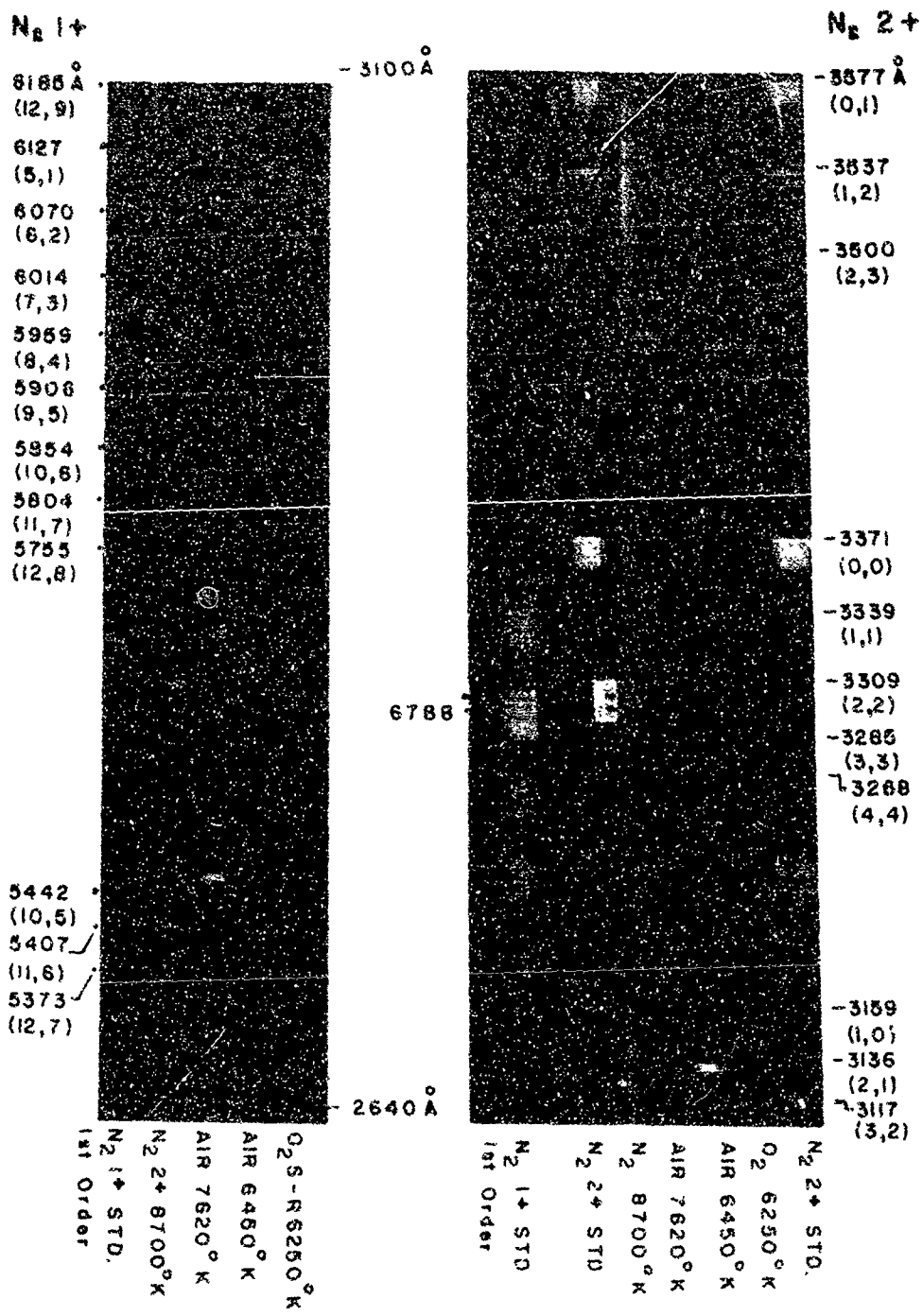

Fig. 9 Meinel Spectrograms of Shock-Heated O_2, Air, and N_2, 2[illegible] Å - 3[illegible] Å

the NOβ and NOγ transitions, and apparently the $N_2(1+)$ transition, and for the purpose of determination of rotational line profiles discussed in Section 5 of this report.

(2) Air Data for 6450°K and 0.74 ρ_o

Figure 10 shows the results of two detailed SACHA calculations of the spectral emissivity per 7.3 cm pathlength for heated air at 6450°K and 0.74 ρ_o for the wavelength range of 3425 Å to 3395 Å (29,197 cm^{-1} to 29455 cm^{-1}) using the NO(β) f-values of 0.008 and 0.0015 for curves (a) and (b), respectively. These curves are to be compared with the densitometer trace for the same wavelength region of the Meinel spectrogram for shock-heated air at 6450°K and 0.74 ρ_o, curve (c), and with the O_2 - S-R emission spectrogram, curve (d), for a shock in pure oxygen for the reflected shock condition of 5450°K and 1.2 ρ_o. The tick marks on the lower abscissa scale indicate the wavelength identifications of the rotation-line structure for the O_2 S-R system, curve (d), in terms of the vibration transitions (v',v") to which they belong shown at lower righthand corner of the figure. The wavelength scale is the same for all four curves. The magnitude of the ordinates on the densitometer traces are neither comparable with each other nor with the absolute emissivity scale, upper left, as calculated by the SACHA code. The figure was set up for the main purpose of showing the results of attempts to observe the NO lines in the air data, curve (c). As discussed above, the NO structure dominates the SACHA calculations for air at 6450°K when the 0.008 f-value for NOβ is used, Fig. 5(c) and Fig. 10(a), and should be of comparable intensity to the O_2 S-R lines when Bethke's f-values are used in the air calculation, Fig.10(b) and Fig. 6(a) and (c). Comparison of the two densitometer traces for air and the O_2-(S-R) in Fig.10(c) and (d), respectively, shows that the overall look and relative magnitude of the rotational structure of the two experimental traces are alike and that with only one or two exceptions all peaks in the air data, curve (c), have corresponding peaks in the O_2 S-R data, curve (d). The exceptions, i.e., additional lines observed in the air data but not in the O_2 data, indicated by [illegible] marks (') on the air data, can conceivably be accounted for in the [illegible] K difference in the rotational temperature distributions for 6450° and [illegible]. Such effects have been observed in comparison of [illegible] different thermodynamic states in pure oxygen.

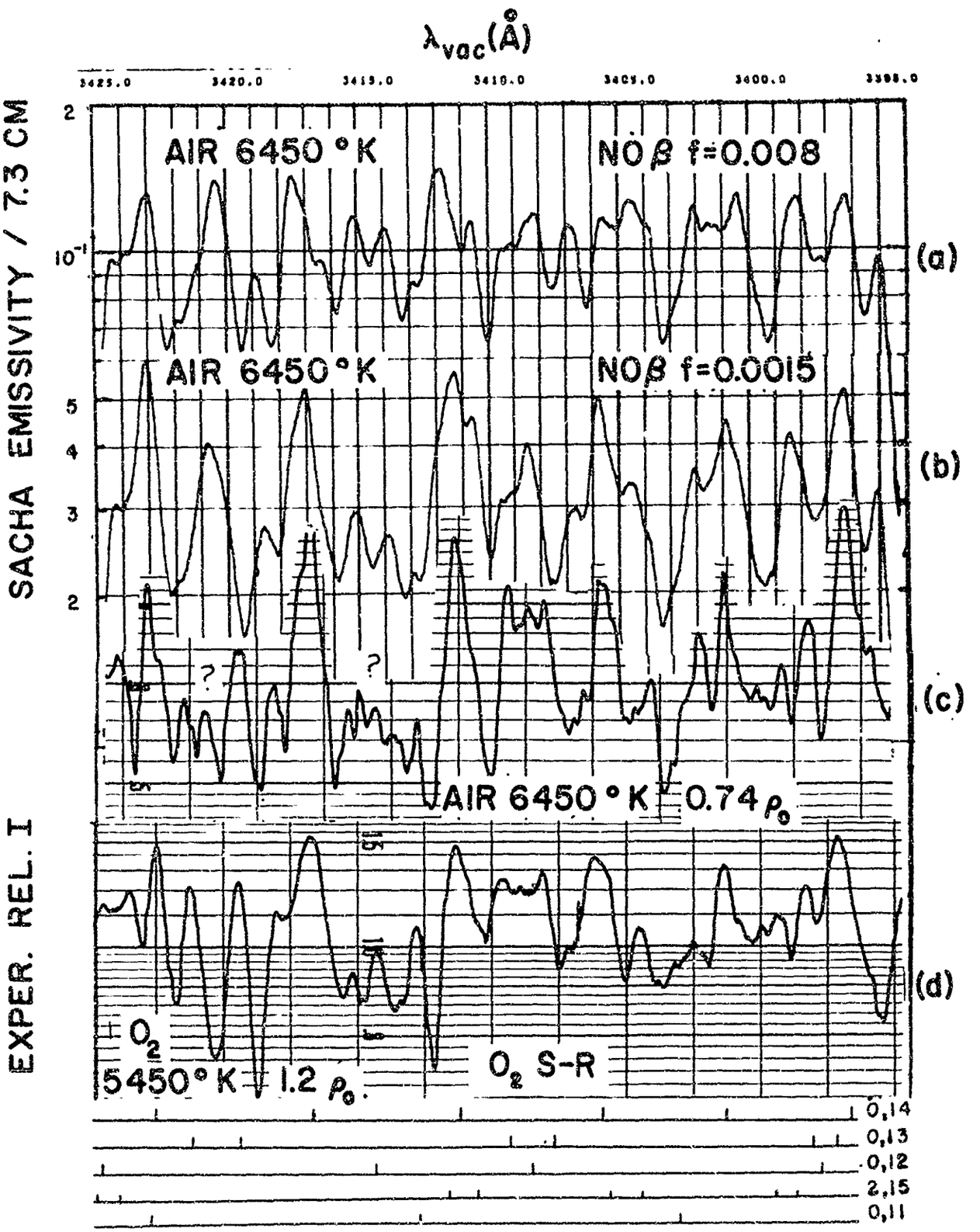

Fig. 10 Experimental-SACHA Comparisons for Air at 6150°K

The two exceptions are not sufficient in number to indicate that the NOβ and γ lines are actually contributing appreciably if any to the rotational line structure for this condition in heated air. Further these results would indicate that Bethke's f-value for the NOβ system of 0.0015 expected to make the main NO contribution in this wavelength range is at least a factor of two too high, i.e., an upper limit of 0.0008 for the NOβ f-value can be set on the basis of our failure to observe the NO lines in this comparison. Careful visual examination of these same data for air and O_2 for the range of the Meinel plates from 5000 Å to 2400 Å, Fig. 9, revealed no lines attributable to either the NOβ or NOγ systems, indicating that Bethke's f-value of 0.0022 for the NOγ system is also too high.

(3) Air Data for 7620°K and 0.85 ρ_o

Figure 11 shows a comparison of the SACHA calculations of the emissivity per 7.3 cm of pathlength with two different NOβ f-values, 0.008 and 0.0015, curves (a) and (b), respectively, for the heated air condition of 7620°K and 0.85 ρ_o in the wavelength region of the $N_2(2+)$ 3371 Å (0,0) band head. Curve (c) shows the densitometer trace of the Meinel spectrogram for shock-heated air for 7620°K and 0.85 ρ_o. Curve (d) is the densitometer trace for this wavelength region for the reflected shock condition in prepurified nitrogen of 9500°K and 0.124 ρ_o. The disruption in the normally orderly appearance of the $N_2(2+)$ structure is around 3360 Å, curve (d), caused by the broad diffuse band head of the NH (0,0) band erratically observed in shocks in N_2 caused by either a failure to close the Meinel shutter before the hydrogen in the combustion driver gases appeared in the field of view of the spectrograph or possibly by a small hydrogen gas impurity that is always present in the Matheson prepurified nitrogen. The appearance of the NH head in curve (d) makes it necessary to make the comparison with the air data in the wavelength region 3355 Å to 3345 Å to the right of the NH. All the lines in the experimental air data, curve (c), can be attributed to $N_2(2+)$ lines seen in curve (d) for N_2 data. Comparison of the experimental air data (c) with the SACHA calculations (a) and (b) does not show the NO structure, curve (a), which perturbs the orderly $N_2(2+)$ "picket-fence" appearance. This NO structure is still apparent in SACHA curve (b) but does not appear in the experimental air data, curve (c).

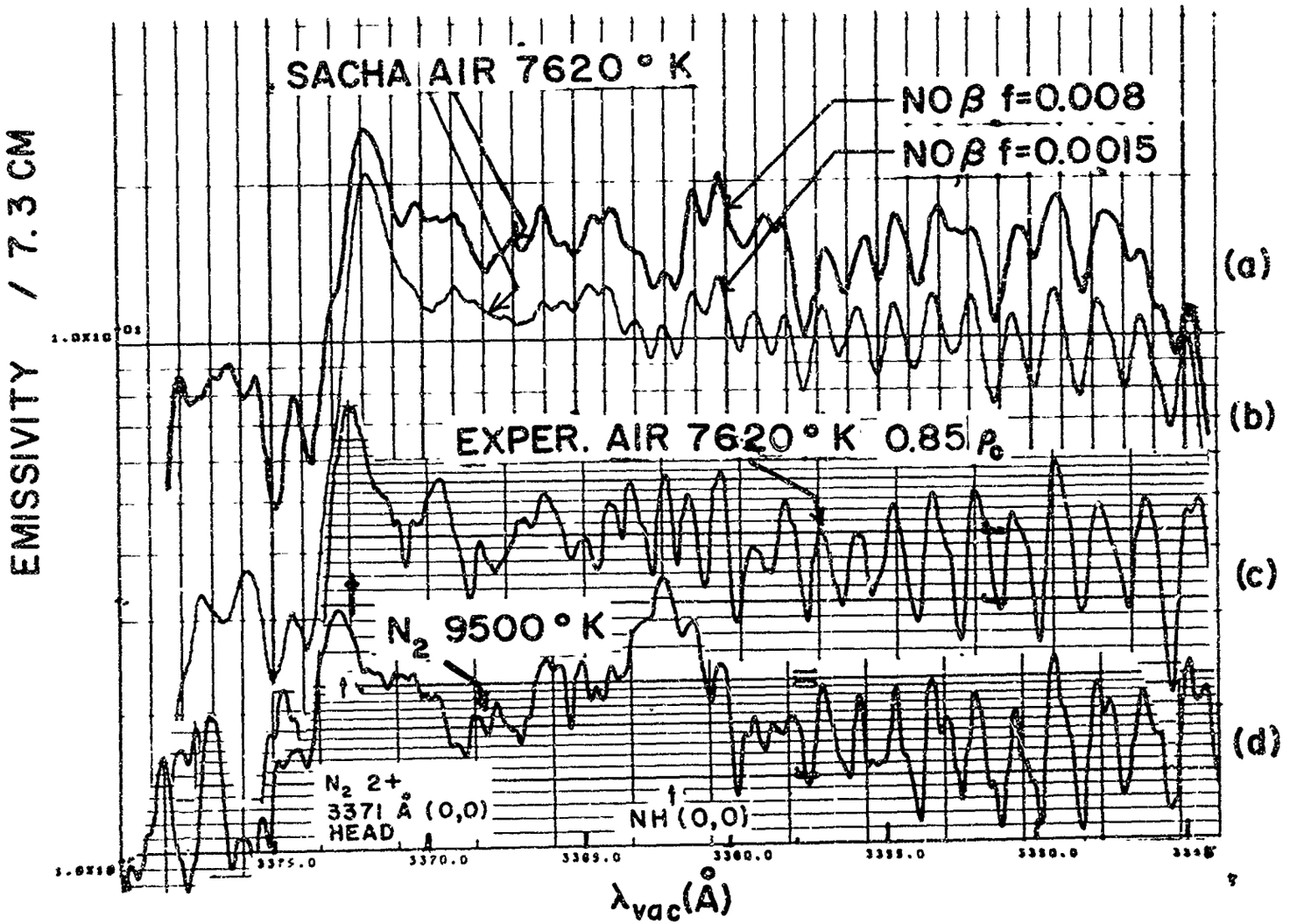

Fig. 11 Experimental-SACHA Comparisons for Air at 7620°K

d. Conclusions, NO Study

The same conclusions regarding NO emission can be drawn for the heated air condition of 7620°K and 0.85 ρ_o as drawn for the air at 6450°K and 0.74 ρ_o, namely, that the NO β f-value of 0.008 presently used in the SACHA code is at least an order of magnitude too large and should be revised downward accordingly. The f-value of 0.0025 for the NO γ system is probably too high because of our failure to positively identify its structure in the air data below 3000 Å. The accuracy of these SACHA-experimental comparisons depend on the accuracy of the f-values of the O_2 S-R and the N_2 (2+) systems presently used in the SACHA calculations. However, failure to observe the NO β and NO γ systems in comparison of the experimental air spectra with those for pure O_2 and N_2 for both these conditions is indeed a fact regardless of the relative f-values of the N_2, O_2 and NO transitions under study. The spectral data for shock heated NO looked no different than that for air for the same temperature-density range. An equilibrated shock-heated NO gas sample would exhibit the same radiation characteristics as a fifty-fifty mixture of N_2 and O_2 at comparable temperatures and densities. Failure to observe the NO systems in heated air spectra could have been due to failure to form the calculated NO concentration in the excited states of interest; however, such is not the case for shocks with NO as the starting gas instead of the O_2 and N_2 mixtures. It can be concluded from failure to observe any lines due to the NO β and γ systems in the comparisons of these high resolution spectra that the Bethke f-values of 0.0015 and 0.0022 for NO β and γ transitions, respectively, represent upper limits and in all likelihood are at least a factor of two too high. Since we did not observe the NO lines we cannot ascribe new values for the oscillator strengths, but it does appear that NO must be relegated to a position of relative unimportance as a contributor to air opacity on the basis of these comparisons.

5. ROTATIONAL LINE SHAPES

(a) Line Widths and Collision Cross Sections

The application of recently developed techniques such as the LMSC SACHA code for computing the spectral emissivity of heated air depends significantly on a knowledge of rotational line profiles. The broadening of spectral lines of atoms and molecules has been the subject of a number of thorough reviews during the last decade (Refs. 19, 20, 21, and 22). None of these reviews has, however, been specifically concerned with the optical spectra of air molecules. A quantum theoretical calculation of the line width parameters determining these profiles is in principle possible and will probably be undertaken eventually. At present the state-of-the-art is not sufficiently advanced to warrant that approach. One does have, however, a fairly good understanding of the physical causes of line broadening and there are several theories, valid under diverse conditions, which take these causes into account. The formulas obtained from these theories have been found to represent experimental data on atomic lines quite well. The same formulas with minor modifications apply to those molecular lines which involve electronic transitions. To begin with, all lines have a natural width because of the finite duration of radiative processes. Under conditions of interest to us, this is always overshadowed by other effects. Another cause of line broadening is the Doppler effect which is well understood and presents no serious problems. Finally there is the broadening due to collisions with the other particles in the gas and this is where most of the difficulty arises. Below the temperature range where air contains enough electrons and ions to cause Stark broadening there is a host of collisions with neutral particles which give rise to various types of pressure broadening. The impact theory for line broadening due to collisions introduces an "optical collision diameter" α_c from which one calculates a line width $\Delta\nu$

$$\Delta\nu = N\alpha_c^2 v \qquad (1)$$

where N and v are the density and velocity of the perturbing particles.

In the equilibrium gas samples of interest here the number density and the kinetic velocity of the radiating particles and of the perturbing particles are calculable quantities. It can be shown from simple kinetic theory that the half-width $\Delta\nu$ in units of cm^{-1} increases linearly with collision frequency of the radiating particle. The optical diameters $\alpha_{mol\text{-}mol}$ and $\alpha_{mol\text{-}atom}$ are related to the half-width of a rotational $\Delta\nu$ line radiated by a molecular specie in collision with similar molecules of number density N_{mol} and with atoms N_{atom} of the dissociated molecule in gas at equilibrium temperature T by

$$\Delta\nu = 2\sigma = \frac{2}{c}\sqrt{\frac{kT}{\pi m_{mol}}}\left(2\,\alpha^2_{mol\text{-}mol}\,[N_{mol}] + [N_{atom}]\,\alpha^2_{mol\text{-}atom}\sqrt{\frac{2m_t}{m_{atom}}}\right) \quad (2)$$

where σ in cm^{-1} is half the width of the line, $c = 3 \times 10^{10}$ cm sec^{-1}, k is the gas constant $= 1.38 \times 10^{-16}$ erg. deg^{-1}, m_{mol} and m_{atom} are the mass in gm of the radiating molecule and the colliding atom, respectively, and $[N_{mol}]$ and $[N_{atom}]$ are the particle concentrations in particles per cm^3 of the molecule and the atom, respectively. The relative magnitude of the first term in the parentheses involving the molecular concentration can be made small compared to the second term involving the atom concentration by working with gas samples with a high degree of dissociation. For such conditions it is not necessary to know the molecule-molecule collision diameter $\alpha_{mol\text{-}mol}$ (first term) and one can ignore the first term and solve directly for the molecule-atom collision diameter, $\alpha_{mol\text{-}atom}$. Once this molecule-atom diameter is known, then it is possible to study rotational emission lines for gas conditions with lower degrees of dissociation for which the first term in Eq. (2) becomes important, and thus obtain the molecule-molecule collision diameter, $\alpha_{mol\text{-}mol}$. Such a range of areas of study can be achieved for O_2 and N_2 by working in the high-temperature, shock-heated molecular-emission regime, i.e., temperatures greater than 7000°K for high degrees of dissociation of O_2 and N_2 and less than 7000°K for lower degrees of dissociation. The density ρ_5 is determined by the requirement of optically thin gas samples in the centers of the rotational lines under study and to some extent by the capabilities of the shock tube in production of these thermodynamic

conditions and of the Meinel spectrograph, Section 3(b), in recording the rotational emission spectra with sufficient photographic-plate density.

All of this discussion has assumed that collision broadening of the rotational levels by rigid-sphere, neutral particles is the dominant mechanism in the determination of the rotational line shapes, and, indeed, it appears that it is possible to record the O_2 (S-R) and the $N_2(2+)$ band systems for such conditions. However, such is not the case for the $N_2^+(1-)$ systems. This molecular ion is only formed in equilibrium in sufficient quantities to be recorded in emission for conditions where the N^+ and electron concentrations are greater than about 10^{16} cm^{-3}. The simple kinetic collision theory just expounded undoubtedly does not apply to the perturbation of the rotational levels of a positive ion by the microfields of the atomic ions and electrons in the surrounding gas.

b. Experimental-SACHA Comparisons of Rotational Intensity Envelopes

High wavelength resolution (0.2 Å) emission spectrograms of molecular band systems for shock-heated equilibrium oxygen and nitrogen have been recorded with the Meinel spectrograph Fig. 9, (Refs. 4, 5 and 16). These high-temperature rotational-vibrational bands exhibit rotational-line intensity envelopes extending to rotational quantum numbers greater than J = 120. The N_2 First Negative 3914 Å (0,0) band recorded for 12,000°K and one eighth normal density in shock-heated nitrogen has been analyzed for line frequency position as a function of J value. The first two rotational constants B_0 and F_0 of Child's were confirmed by this analysis and a new value obtained for the third constant H_0 for the v' = 0 upper vibrational level by Buttrey and Gibson (Ref. 4). In general, in spectra of this sort, it is not possible to find a single isolated rotational line whose shape we can investigate, as was possible, for example, in the case of the atomic oxygen line at 4368 Å whose Stark-broadened profile was found to fit a Lorentz dispersion shape (Ref. 4). Instead, the determination of rotational line shapes and widths is complicated by overlapping of lines in and near the peaks due to splitting of the rotational levels and further is confused by lines from overlapping branches of the same vibrational transition as well as by lines from other vibrational transitions. The

experimentalist can determine at best the "apparent" half-width of a "clump" of rotational lines using an intensity level for the continuum which must be chosen arbitrarily because of overlapping of the wings of the conglomerate of rotational line profiles. Our best knowledge of the line frequency locations and the splittings of the lines which form the clumps involves inaccuracies which are comparable to the half-widths of the individual split components of interest, particularly for the lines of high rotational quantum numbers exhibited in the high-temperature shock spectra. In the case of the O_2 S-R band systems, lines from at least ten vibrational transitions (v',v") make significant contributions in any selected 20 Å bandpass, and errors in the relative transition probabilities as well as line frequency positions play a role in the interpretation of the line clumps in terms of the profile of a single line.

In an attempt to solve these problems a series of detailed comparisons of the experimental spectral intensity in selected wavelength bandpasses have been made with the detailed rotational line-intensity envelopes calculated with the SACHA IBM 7094 digital-computer program (Ref. 14) for the experimental thermodynamic conditions. The SACHA program contains an atlas of the parameters of the six molecular transitions listed in Table 1 such that it can generate a theoretically predicted rotational-line intensity envelope in any spectral region from about 100,000 Å to 2,000 Å for any specified thermodynamic condition of interest in the molecular regime. It employs a Lorentz line shape with a variable half-width input, the best experimental f-values for the molecular transitions available at the time the code was set up, Table 1, the relative transition probabilities or Franck-Condon factors of Nicholls (Refs. 23, 24 and 25) for each vibrational transition (v',v"), and the rotational constants from various sources in the literature for the prediction of the line frequencies. The code accounts for rotational level splitting due to Λ doubling in the $N_2(2+)$ transition, for example, but does not account for splitting due to electron spin interactions in the cases of the $O_2^+(1-)$ and the O_2(S-R) transitions. Discrepancies of about one to six wavenumbers in the frequency position of rotational lines at $J \approx 30$ have been found with those in frequency atlases

in the published literature for each of these three transitions. This is not a serious error in most opacity calculations for which the code was designed, but it is serious in the comparison of detailed rotational-line-intensity structure with experimental data for the determination of line shapes and widths. In order to overcome these discrepancies in line frequencies special SACHA type calculations have been made for the $N_2^+(1-)$ system using the published frequencies (Refs. 4 and 26) which also include frequencies of the split components, resulting in considerably better fit with the experimental envelope. All attempts to record the emission spectra of the NOβ and NOγ systems in shock-heated air and in shock-heated NO failed, Section 4, nor have we observed the N_2 First Positive System. Therefore, of necessity we must limit our discussion and our study of line shapes to the three rotational vibrational systems observed experimentally in high-resolution spectrograms, namely, the N_2^+ (1-), the $N_2(2+)$ and the O_2 S-R systems. The discussion which follows summarizes the work performed this past year on each of these three band systems, and the problems encountered, and it outlines the nature of future efforts in the study of this very difficult problem of rotational line shapes.

(1) N_2^+ First Negative System, Rotational Line Shapes

As a first step in overcoming these inadequacies of the SACHA code, a revised frequency atlas including splitting (Refs. 4 and 26) has been employed in SACHA calculations of the intensity structure in a 20 Å bandpass for the strong 3914 Å (0,0) band head of the $N_2^+(1-)$ system. Calculations were made using this revised atlas for the lines of this vibrational transition only for a range of widths in order to compare with the spectral intensity obtained for the optically thin condition of 9500°K and 0.124 normal density in shock-heated nitrogen. The comparison of the calculated intensity profile for a width at half maximum of 2 cm^{-1} with the experimental data is shown in Fig. 12. The upper curve is the SACHA calculation of the emissivity for a 7.3 cm pathlength plotted as a function of frequency for the range 25,525 cm^{-1} to 25,625 cm^{-1} for the temperature of 9500°K and an N_2^+ concentration of 1.7×10^{15} particles cm^{-3}. The lower curve is a densitometer trace of the experimental data. Analysis of the experimental

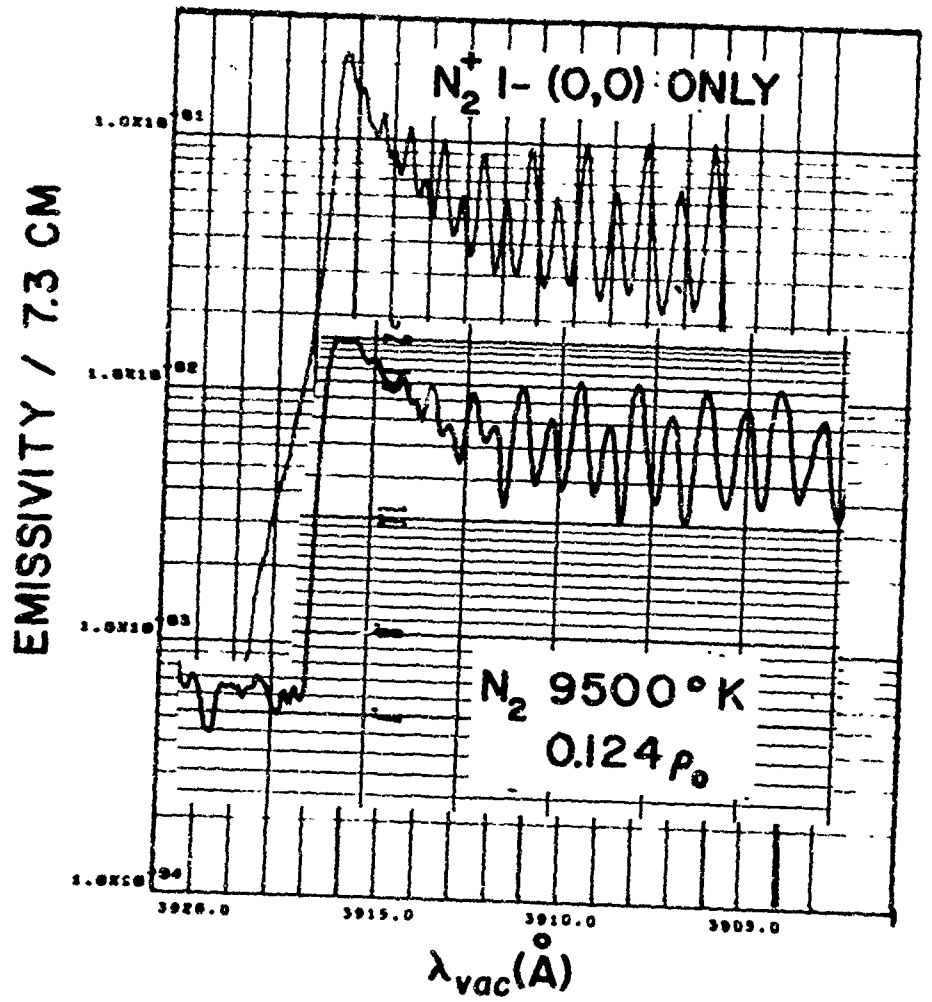

SACHA
Line width = 2.0 cm^{-1}
Bennett and Dalby f/value = 0.0348
T = 9500°K
N_2^+ = 1.7×10^{15} cm^{-3}

EXPERIMENTAL
Instrumental line width = 0.9 cm^{-1}
Line width from fit with
SACHA in pk/min analysis = 1.94 cm^{-1}

$[N_2^+] = 1.7 \times 10^{15}$
$[N_2] = 6.2 \times 10^{17}$
$[N] = 6.9 \times 10^{18}$
$[N^+,e] = 3.45 \times 10^{16}$

Fig. 12 Comparison of Special SACHA Calculation of Spectral Emissivity per 7.3 cm Pathlength for the N_2^+ 3914 Å (0,0) Band Head with Experimental Shock-tube Data, for Pure N_2 at 9500°K and 0.124 Normal Density

data using appropriate emulsion calibration curves was made such that the ratio of the peak intensity to the minimum intensity were determined for the structure shown, J(P) = 26 to 33 superimposed on J(R) = 0 to 4. These were compared with similar peak-to-minimum ratios as a function of half-width calculated with the SACHA code using the revised atlas, the results of which calculations are shown in Fig. 13. A best-fit to the experimental data was found for the width at half maximum of 1.9 cm^{-1}. This value is an average of the individual widths for each J-value obtained by reading the width from the appropriate curve, Fig. 13, for the experimental peak-to-minimum values. These individual widths thus obtained are listed in Table 3 for J-values of the P-branch lines included in each peak or clump of lines. These widths represent

Table 3

RESULTS OF EXPERIMENTAL-SACHA PEAK-TO-MINIMUM AND HALF-WIDTH ANALYSIS, N_2^+(1-) 3914 Å (0,0) BAND HEAD

J(P)	Exper. Pk/Min Ratios	Widths at Half Maximum (cm^{-1})
26	2.15	2.46
27	2.67	1.58
28	3.46	2.02
29	2.36	1.68
30	4.20	1.99
31	3.12	1.70
32	4.19	2.14
33	3.24	1.94

the total width of the Lorentz profile at half peak intensity for a single split rotational line component. The spread of the widths is sufficiently small that one can conclude that the Lorentz dispersion shape is appropriate to describe the excited-state rotational energy level for this thermodynamic condition. This work needs to be extended over a wider range of widths as a function of temperature and density.

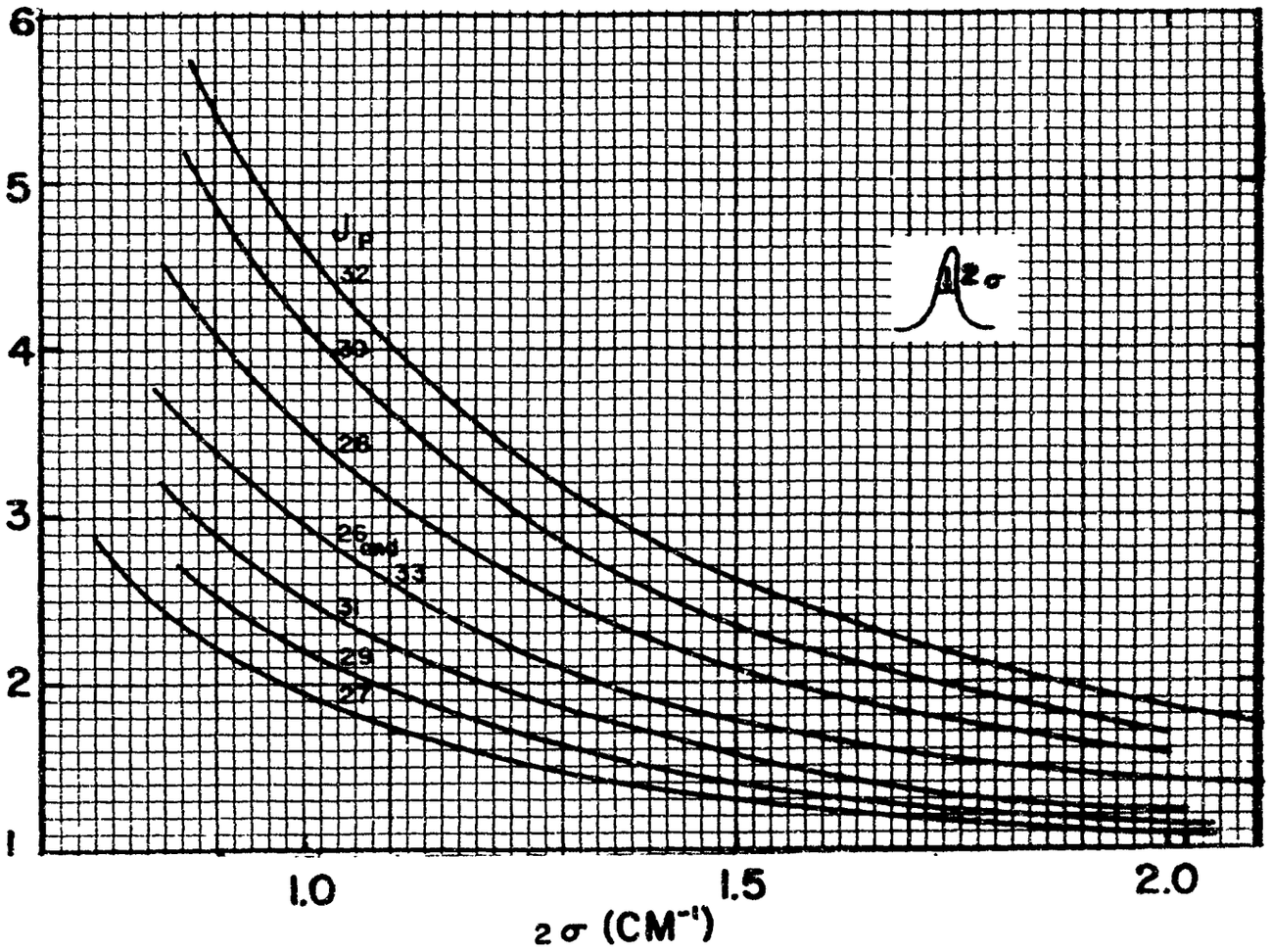

Fig. 13 SACHA Calculation of the Ratio of Peak-to-Minimum Intensity Versus Line Width for Rotational Line-Intensity Structure in the N_2^+(1-) 3914.4 Å (0,0) Band Head Using the Frequency Atlas of Childs

(2) O_2 Schumann-Runge System ,Rotational Line Shapes

The O_2 S-R system is considerably more troublesome since seven or more vibrational bands make intensity contributions of comparable magnitude in any narrow frequency range - some with lines of high J-values and some with low J-values. Errors in rotational line frequencies and the failure to include the asymmetrical spin-splitting in the present SACHA program for O_2 S-R make it practically impossible to find a general fit with the experimental intensity envelope for any selected frequency bandpass.

Figure 14 shows a comparison of the calculated intensity envelope using the present SACHA program (dotted curve) with the experimental intensity envelope (solid curve) for the optically-thin, reflected-shock condition of 8400°K and one-third normal density in pure O_2 for the frequency range of 29,390 cm^{-1} to 29,450 cm^{-1}. Absolute emissivity as calculated by the SACHA code for the O_2 (S-R) lines using a 6 cm^{-1} width is plotted on the vertical axis. Normalization of the experimental intensity envelope to the SACHA curve was made for the peak of the seemingly isolated line "clump" labelled (0,14) R 27, P 23. Notice that the SACHA calculation (dotted curve) predicts another line clump in the middle of the frequency range which failed to materialize in the experimental data (solid curve).

The bar graph under the two curves shows the SACHA-calculated integrated intensity as a function of frequency position for each rotational line listed in the SACHA frequency atlas for this bandpass. Plotted on the scale below the graph are the frequency positions for the strong (0,14), (0,13) and (2,15) transitions taken from the atlas of Lochte-Holtgreven-Dieke (Ref. 27) from an emission study of the O_2 S-R spectrum from which atlas identification of the experimental curve was determined. Comparison of these line frequencies with those on the bar graph for the same lines shows gross discrepancies of 6 cm^{-1} and more in frequency position as calculated by the SACHA codes versus the published data, which can possibly account for the misplaced SACHA clump in the middle of the bandpass. The shift in the peak position of about 1 cm^{-1} of the line clump labelled (0,14)

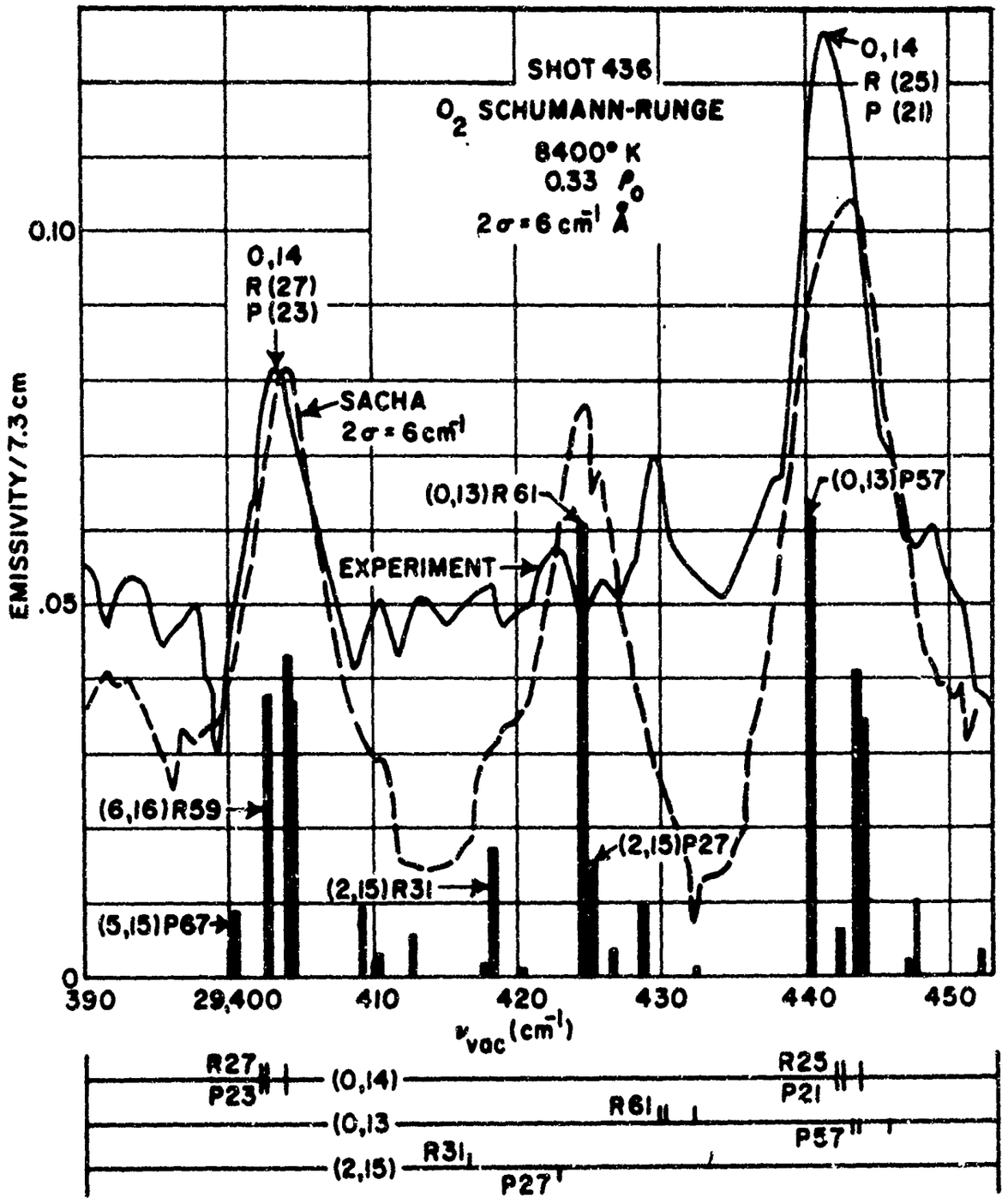

Fig. 14 Experimental-SACHA Comparison of Rotational-Line Intensity Envelopes, O_2 Schumann-Runge System, 8400°K and 0.33 ρ_o, 29, 390 cm^{-1} to 29,450 cm^{-1}

R (27) P (23) is attributable to the fact that the SACHA code does not include spin splitting of the lines into three asymmetrically placed line components as discussed previously.

In spite of the poor overall fit of the intensity envelopes in this bandpass, Fig. 14, a peak-to-minimum analysis similar to that for the N_2^+ 3914 Å (0,0) band head has been made for the seemingly isolated line clump labelled (0,14) R (27) P(23). Notice that the SACHA calculation includes a (6,16) line of about equal intensity to the P and R components of the (0,14) system and displaced to shorter frequency by an amount equal to the separation of the P and R components (about 1 cm^{-1}). The experimental SACHA peak to minimum analysis for this clump yielded a preliminary width of 6 cm^{-1} for each line corresponding to an O_2-O collision diameter of 9 Å or a cross section of 2×10^{-14} cm^2. This width was used in the SACHA calculation of the intensity envelope shown in Fig. 14, (dotted curve). In spite of the apparent fit for this width, the validity of such a comparison is questionable. It is not clear that the (6,16) line in this clump, for example, has either an intensity of this magnitude or that it appears at this frequency position in the experimental data. And, of course if it did, the SACHA calculation has not included spin splitting into 3 lines for each P and R component, which, if we could isolate a single split P component, for example, and compute its profile, we would observe an asymmetric profile with a hump on the long frequency side corresponding to the unperturbed level, and a peak displaced about 1.25 cm^{-1} corresponding to the other two split components which lie relatively close together.

What is planned for this complicated system is to set up on a piecemeal basis a revised frequency atlas using published frequencies of the stronger (v',v") transitions and then compare the calculated and experimental envelopes to discover what other important lines appear in the bandpass in the high-temperature, high J-value shock data. Since there is no published frequency data on the (6,16) transition we plan to omit it from our first calculations. Somehow, we have to make the calculated clump in the middle of the frequency bandpass, Fig. 14, disappear, whether

it be by revision of the Franck Condon factors ($q_{v',v''}$) and/or by successive revisions of the wavelength frequency atlas. This needs to be done for several selected bandpasses which include seemingly isolated clumps of rotational lines amenable to the rotational line shape study. Then spin splitting will be included and peak-to-minimum analyses made to investigate line shapes of individual components.

(3) N_2 Second Positive System, Rotational Line Shapes

Two bandpasses in the band head region of the strong 3371 Å (0,0) and 3159 Å (1,0) transitions have been under study. The SACHA code includes the Λ-doubling type splitting of the rotational levels for these band systems. However, gross errors in line frequency positions must be corrected before line shape studies can proceed.

These vibrational band systems are strong relative to others contributing line intensity in the vicinity of the band origins and therefore should lend themselves rather nicely to the line shape study.

c. Discussion of Line Shape Studies

In the previous discussion we have outlined the efforts from which we hope to determine the widths and shapes of rotational lines emitted by the O_2, the N_2 and the N_2^+ in collision with molecules and under the influence of other constituents, both molecules and atoms existing in the high-temperature equilibrium gas samples. In general we have been able to study gas samples which are optically thin in the centers of the rotational lines and for which gas samples we can be reasonably assured of attaining equilibrium conditions in reflected shock gas samples. The widths of the rotational lines are determined by the frequency of collisions of the radiative molecule with other molecules and atoms in the gas sample. This makes interpretation of the derived widths in terms of a molecule-atom or a molecule-molecule cross section a complex problem unless it is possible to show that the chance for the molecule to collide with an atom is at least 50 times greater than its chance to collide with another molecule. The high-temperature emission studies of O_2(S-R) lines, Sec. 5b(2) were made for conditions for which the dissociation of molecular

species under study was essentially complete (>95%) and for which the molecule-atom collision cross sections can be derived from the line widths without resorting to assumptions as to the ratio of the molecule-molecule cross section to the molecule-atom cross section. The value of 2×10^{-14} cm^2 obtained for the O_2 - O collision cross section for the O_2(S-R) line width of 6 cm^{-1} at 3400 Å for the condition of 8400°K and 0.33 ρ_o in oxygen is subject to change when the problems of rotational line frequency position and of Franck-Condon factors $q_{v',v''}$ have been resolved; however, this value of 2×10^{-14} cm^2 undoubtedly represents an upper limit for the O_2 - O optical collision cross section. When we have derived the molecule-atom cross section from these line width studies, we will then be able to determine the molecule-molecule collision cross sections by line width investigations for conditions with smaller degrees of dissociation for which both types of collisions contribute to the broadening of the rotational levels.

This simple kinetic theory reasoning applies very nicely to the O_2(S-R) line studies and possibly to the N_2(2+) line studies. However, in the case of the N_2^+(1-) system it is not possible to record these bands in emission except for conditions of high atom-ion and electron densities ($N^+ \geq 10^{16}$ cm^{-3}), and of course for high degrees of N_2 dissociation. The molecular ion N_2^+ is always a minor constituent in the gas samples and, although its rotational lines lend themselves most easily to line shape studies, interpretation of the widths in terms of simple kinetic collision cross sections is probably not valid. Interpretation of the line width of 1.9 cm^{-1} obtained for the N_2^+(1-) 3914 Å (0,0) for the condition of 9500°K and 0.124 ρ_o in nitrogen (Fig. 12), from the peak-to-minimum analysis in terms of a collision cross section is not possible at this time. Stark-broadening of the levels due to the microfields of the surrounding ions and electrons will undoubtedly be an important broadening mechanism.

6. NITROGEN CONTINUUM MEASUREMENTS IN THE MOLECULAR REGIME

a. Spectroscopic Background

In the range of reflected shock conditions above 9000°K and about one-eighth ρ_o in pure nitrogen where a visible emission continuum is observed simultaneously with the N_2 (2+) and the N_2^+ (1-) band systems, three processes and possibly four can contribute to the spectral continuum intensity. The relative contributions of these processes vary in a complicated manner as the temperature and particle densities change. The possible contributors are

(1) $N^+ + e \leftrightarrow N + h\nu$, free-bound,
(2) $N^+ + e \leftrightarrow N^+ + e' + h\nu$, free-free,
(3) $N + e \leftrightarrow N + e' + h\nu$, free-free, and
(4) $N + e \leftrightarrow N^- + h\nu$, free-bound processes.

The purpose of the absolute intensity measurements reported here is to extract from the total the intensity due to the first process of ion-electron recombination and to compute the recombination cross section. From detailed balancing arguments the photoelectric cross sections for excited states of atomic nitrogen may be obtained.

The procedure used here is to compute the spectral intensity of the free-free radiation (2) of the electron in the field of the positive ion from Karzas and Latter's cross sections (Ref. 18); to assume the free-free radiation for the electron in the field of the neutral atom to be negligible; and to check on the experimental N^- photodetachment cross sections of Boldt (Ref. 12). The intensity remaining was used to obtain the photoelectric cross sections for process (1). Thus the accuracy of the resultant cross sections depends on the accuracy of the subtracted components as well as on the assumption that the calculated Hugoniot equilibrium concentrations of the various species are actually achieved in the measured intensity plateaus of 5 to 20 μsec duration. For the reflected shock conditions of interest overshoots have

been observed in the N_2^+ (1-) radiation signals followed by plateaus which we think is the equilibrium signal (Ref. 4). It is these equilibrium plateaus which are reported here.

The transmission at a given wavelength λ of a gas sample of pathlength x is

$$T_\lambda = \frac{I_\lambda}{I_\lambda^o} = e^{-\mu_\lambda x} \tag{3}$$

where I_λ^o is the incident intensity at wavelength λ, I_λ the transmitted intensity, and μ_λ the total absorption coefficient per cm. For local thermodynamic equilibrium, Kirchoff's Law holds, and the gaseous emissivity is

$$\epsilon^\lambda_{total} = 1 - e^{-\mu_\lambda x} = \frac{I^\lambda_{em}}{B_\lambda(T_5)d\lambda} \tag{4}$$

where I^λ_{em} is the emission intensity at wavelength λ and $B_\lambda(T_5)d\lambda$ is blackbody intensity at wavelength λ for the reflected shock temperature T_5. For $\epsilon^\lambda_{total} \leq 0.15$, $\epsilon^\lambda_{total} = |\mu_\lambda x|$. I^λ_{em} is the quantity measured for selected wavelengths between 3429 Å and 6080 Å. The total emissivity is computed for each wavelength, and then corrected for self-absorption if ϵ^λ_{total} is greater than 0.15.

Thus

$$\epsilon^\lambda_{total}\ (\text{corrected}) = |\mu x| = \epsilon^\lambda_{N(PE)} + \epsilon^\lambda_{ff(+)} + \epsilon_{N^-(PD)} + \epsilon_{ff(neutral)}. \tag{5}$$

The purpose of the continuum intensity measurements is to obtain the spectral emissivity for the nitrogen photoelectric process $\epsilon^\lambda_{N(PE)}$ for a range of temperature between 9,000 and 12,000°K.

The frequency distribution of intensity from which we will compute $\epsilon^\lambda_{ff(+)}$ due to the free-free energy transitions of the electron in the field of the positive ion versus frequency as given by Karzas and Latter (Ref. 18) is

$$\langle I \rangle_\nu\, d\nu = \frac{2^5 \pi e^6}{3\ hmc^3} Z^2\ N_e\ N_{ion} \left(\frac{2\pi kT}{3m}\right)^{1/2} du\ e^{-u} \left\langle g(u,\gamma^2) \right\rangle \frac{ergs}{sec\ cm^3} \tag{6}$$

where

$$u = \frac{h\nu}{kT}, \qquad \gamma^2 = \frac{Z^2 R_y}{kT},$$

and R_y is the Rydberg constant in cm^{-1} for the ion, T is in degrees Kelvin, and e and m are the charge and mass of the electron and Z the charge on the ion, 1 in our case. $\langle g(u,\gamma^2) \rangle$ is a temperature averaged Gaunt factor for the electron in a Coulomb field, which is equal to 1.22 and essentially constant for the temperature and wavelength range investigated here. The classical rate of bremsstrahlung production by Kramers (Ref. 28) has been increased by those average Gaunt factors which have been obtained as functions of temperature for a Boltzmann distribution of electron energies over a wide range of photon energies. Only a small portion of this range of photon energies is under investigation here, namely, about 2 eV to 4 eV.

It is assumed that the emissivity contribution of the free-free transitions of the electron in the field of the neutral atom $\epsilon_{ff(neutral)}$ is negligible, and after subtracting the $\epsilon_{ff(+)}$ for free-free transitions in the field of the positive ion the remaining spectral emissivity will be interpreted as due to a combination of the recombination and the photodetachment processes. Boldt obtained values of N^- photodetachment cross sections for the energy range of 2 eV to 3 eV varying smoothly from 0.82×10^{-16} cm^2 to 1.15×10^{-16} cm^2, using an electron affinity of 1.1 eV to compute the equilibrium concentration of N^-. He also used Kramer's (Ref. 28) calculations for the free-free radiation of the electron in the field of the positive ion whereas here the larger cross sections of Karzas and Latter are used.

where

$$u = \frac{h\nu}{kT}, \qquad \gamma^2 = \frac{Z^2 R_y}{kT},$$

and R_y is the Rydberg constant in cm^{-1} for the ion, T is in degrees Kelvin, and e and m are the charge and mass of the electron and Z the charge on the ion, 1 in our case. $\langle g(u,\gamma^2) \rangle$ is a temperature averaged Gaunt factor for the electron in a Coulomb field, which is equal to 1.22 and essentially constant for the temperature and wavelength range investigated here. The classical rate of bremsstrahlung production by Kramers (Ref. 28) has been increased by these average Gaunt factors which have been obtained as functions of temperature for a Boltzmann distribution of electron energies over a wide range of photon energies. Only a small portion of this range of photon energies is under investigation here, namely, about 2 eV to 4 eV.

It is assumed that the emissivity contribution of the free-free transitions of the electron in the field of the neutral atom $\epsilon_{ff(neutral)}$ is negligible, and after subtracting the $\epsilon_{ff(+)}$ for free-free transitions in the field of the positive ion the remaining spectral emissivity will be interpreted as due to a combination of the recombination and the photodetachment processes. Boldt obtained values of N^- photodetachment cross sections for the energy range of 2 eV to 3 eV varying smoothly from 0.82×10^{-16} cm^2 to 1.15×10^{-16} cm^2, using an electron affinity of 1.1 eV to compute the equilibrium concentration of N^-. He also used Kramer's (Ref. 28) calculations for the free-free radiation of the electron in the field of the positive ion whereas here the larger cross sections of Kurzas and Latter are used.

b. SACHA Calculations of Average Emissivity Due to Molecular Lines

The molecular band systems of $N_2(2+)$ (2500 Å - 3800 Å) and $N_2^+(1-)$ (3400 Å - 5300 Å) and possibly the $N_2(1+)$ (5000 Å - 1 μ) radiate simultaneously along with the nitrogen continuum processes just discussed. Both line and continuum processes contribute to the radiation signals from the photomultipliers for the nine narrow wavelength band passes listed in Table 1, Section 2, covering the wavelength range from 3371 Å to 6080 Å. In order to ascertain the magnitude of the spectral continuum intensity for these photomultiplier bandpasses the SACHA code has been used to compute the average emissivity due to the lines only for each wavelength-bandpass. Subtraction of the calculated, average line emissivity from the measured total emissivity yields the continuum emissivity. In general the accuracy of the SACHA calculations of the average of the emissivity due to the lines only in a given bandpass varies directly with the accuracy of the f-values used in the SACHA program, Table 1, Section 2, for the three nitrogen band systems making contributions. These absolute intensity measurements of line-plus-continuum radiation for known equilibrium shock conditions serve as a check on the validity of these f-values. The wavelength bandpasses were set up for both on and off the band heads of the $N_2(2+)$ 3371 Å (0,0) and the $N_2^+(1-)$ 3914 Å (0,0) band systems for the purpose of determining the total line-plus-continuum radiation and of checking simultaneously on the validity of the input f-values.

The results of these calculations for the nine wavelength bandpasses, Table 2, Section 3,c, are shown in graph of Fig. 15 which is a plot of the sum of only the line emissivities per 7.3 cm pathlength from all three molecular band systems, i.e. $N_2(2+)$, $N_2^+(1-)$ and $N_2(1+)$, as a function of reflected shock temperatures T_5 for a starting downstream pressure of 1 mm of pure nitrogen in the shock tube. The separate emissivity contributions of these three band systems are listed in Table 4 along with the reflected-shock concentrations of N_2 and N_2^+ appropriate to the various temperatures T_5. It should be mentioned here that the f-value for the $N_2(1+)$ band system of 0.02 used by the SACHA code in this calculation is reputedly too high and a better f-number is about 0.003* which revision is borne out

* Private Communication with W. Wurster.

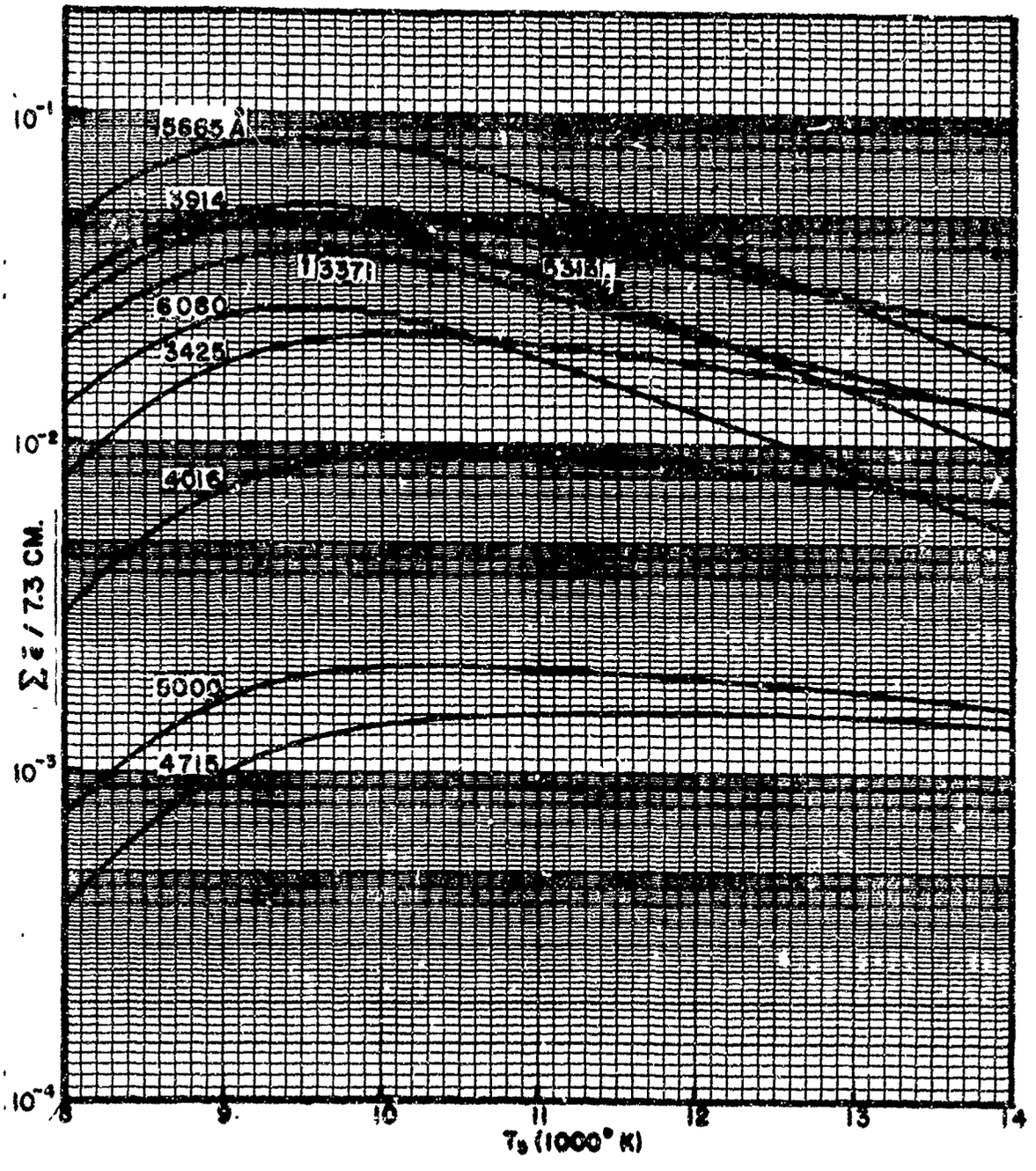

Fig. 15 SACRA Calculations of the Average Spectral Emissivity Due to Molecular Lines for Nine Wavelength Bandpasses Versus Reflected-Shock Temperature T_5 for p_1 = 1 mm N_2

TABLE 4

SACHA CALCULATIONS OF AVERAGE SPECTRAL EMISSIVITY PER 7.3 CM PATHLENGTH DUE TO MOLECULAR BANDS VERSUS REFLECTED-SHOCK TEMPERATURE FOR p_1 = 1 mm N_2 *

Wavelength Bandpass Å	Temp. °K	$N_2(1+)$ $\bar{\varepsilon}$/7.3cm	$N_2(2+)$ $\bar{\varepsilon}$/7.3cm	$N_2^+(1-)$ $\bar{\varepsilon}$/7.3cm	$\sum\bar{\varepsilon}$/7.3cm
3362.4 to 3375.9	6,000	0	6.14^{-4}	4.28^{-5}	6.56^{-4}
	7,000	0	5.04^{-3}	4.76^{-4}	5.52^{-3}
	8,000	0	1.79^{-2}	2.40^{-3}	2.03^{-2}
	9,000	0	3.02^{-2}	5.64^{-3}	3.59^{-2}
	11,000	0	1.99^{-2}	8.23^{-3}	2.81^{-2}
	14,000	0	8.45^{-4}	6.15^{-3}	6.40^{-3}
3414.7 to 3428.1	6,000	0	6.39^{-5}	1.01^{-4}	1.65^{-4}
	7,000	0	7.23^{-4}	1.02^{-3}	1.74^{-3}
	8,000	0	3.27^{-3}	4.76^{-3}	8.03^{-3}
	9,000	0	6.62^{-3}	1.06^{-2}	1.72^{-2}
	11,000	0	5.59^{-3}	1.44^{-2}	1.99^{-2}
	14,000	0	2.16^{-4}	1.04^{-2}	1.26^{-2}
3898.8 to 3922.2	6,000	0	3.56^{-5}	1.41^{-3}	1.45^{-3}
	7,000	0	4.05^{-4}	8.54^{-3}	8.94^{-3}
	8,000	0	1.84^{-3}	2.70^{-2}	2.89^{-2}
	9,000	0	3.75^{-3}	4.45^{-2}	4.83^{-2}
	11,000	0	3.19^{-3}	3.97^{-2}	4.29^{-2}
	14,000	0	1.25^{-3}	1.99^{-2}	2.12^{-2}
4005.8 to 4016.9	6,000	0	2.04^{-5}	3.93^{-5}	5.96^{-5}
	7,000	0	3.22^{-5}	4.17^{-4}	6.52^{-4}
	8,000	0	1.09^{-3}	2.05^{-3}	3.15^{-3}
	9,000	0	2.28^{-3}	4.81^{-3}	7.09^{-3}
	11,000	0	2.03^{-3}	7.08^{-3}	9.10^{-3}
	14,000	0	8.30^{-4}	5.69^{-3}	6.53^{-3}

*Exponents indicate powers of ten.

TABLE 4 (Con't)

Wavelength Bandpass Å	Temp. °K	$N_2(1+)$ $\bar{\epsilon}$/7.3cm	$N_2(2+)$ $\bar{\epsilon}$/7.3cm	$N_2^+(1-)$ $\bar{\epsilon}$/7.3cm	$\sum\bar{\epsilon}$/7.3cm
4710.5 to 4721.8	6,000	0	0	8.02^{-6}	8.02^{-6}
	7,000	0	0	7.98^{-5}	7.98^{-5}
	8,000	0	0	3.96^{-4}	3.96^{-4}
	9,000	0	0	9.58^{-4}	9.58^{-4}
	11,000	0	0	1.51^{-3}	1.51^{-3}
	14,000	0	0	1.31^{-3}	1.31^{-3}
4997.0 to 5017.0	6,000	0	0	1.84^{-5}	1.84^{-5}
	7,000	0	0	1.71^{-4}	1.71^{-4}
	8,000	0	0	7.54^{-4}	7.54^{-4}
	9,000	0	0	1.62^{-3}	1.62^{-3}
	11,000	0	0	2.09^{-3}	2.09^{-3}
	14,000	0	0	1.49^{-3}	1.49^{-3}
5309.4 to 5323.3	6,000	7.78^{-4}	0	3.98^{-6}	7.82^{-4}
	7,000	6.81^{-3}	0	5.18^{-5}	6.86^{-3}
	8,000	2.52^{-2}	0	2.94^{-4}	2.55^{-2}
	9,000	4.34^{-2}	0	7.62^{-4}	4.41^{-2}
	11,000	2.93^{-2}	0	1.28^{-3}	3.05^{-2}
	14,000	9.02^{-3}	0	1.14^{-3}	1.02^{-2}
5655.0 to 5675.0	6,000	1.26^{-3}	0	2.09^{-7}	1.26^{-3}
	7,000	1.17^{-2}	0	3.80^{-6}	1.17^{-2}
	8,000	4.50^{-2}	0	2.68^{-5}	4.50^{-2}
	9,000	7.95^{-2}	0	8.18^{-5}	7.96^{-2}
	11,000	5.66^{-2}	0	1.73^{-4}	5.68^{-2}
	14,000	1.84^{-2}	0	1.91^{-4}	1.86^{-2}

TABLE 4 (Con't)

Wavelength Bandpass Å	Temp. °K	$N_2(1+)$ ε/7.3cm	$N_2(2+)$ ε/7.3cm	$N_2^+(1-)$ ε/7.3cm	$\sum\varepsilon$/7.3cm
6069.0 to 6097.0	6,000	3.16^{-4}	0	1.04^{-7}	3.16^{-4}
	7,000	3.14^{-3}	0	2.26^{-6}	3.14^{-3}
	8,000	1.28^{-2}	0	1.77^{-5}	1.28^{-2}
	9,000	2.36^{-2}	0	5.90^{-5}	2.37^{-2}
	11,000	1.75^{-2}	0	1.43^{-4}	1.76^{-2}
	14,000	5.85^{-3}	0	1.81^{-4}	6.03^{-3}

qualitatively by our measurements to be discussed in the next section. This would effectively reduce the emissivities listed in Table 4 for the $N_2(1+)$ lines by a factor of 0.15 for the wavelength bandpasses for which these band systems are important radiators, i.e., 5300 Å, 5665 Å, and 6080 Å. Since our measured total emissivities for these wavelengths for this range of temperatures are not as large in general as those calculated by the SACHA code, Fig. 15 and Table 3, we have taken the liberty of reducing the $N_2(1+)$ average spectral line emissivities to 15 percent of those listed in Table 4. It is these reduced values which we have subtracted from our total measured emissivities for these wavelengths.

Figure 16 shows the Rankine-Hugoniot calculations of the equilibrium particle densities behind the reflected shock plotted as a function of both reflected shock temperature T_5 and reciprocal incident shock velocity U_s^{-1} in microseconds per ft for the starting downstream pressure of $p_1 \approx 1$mm N_2. The vertical line at 12,000°K indicates roughly the upper limit for the range of reflected-shock conditions under investigation in the nitrogen line-plus-continuum intensity measurements, as well in the rotational line shape studies for the $N_2(2+)$ and the $N_2^+(1-)$ systems.

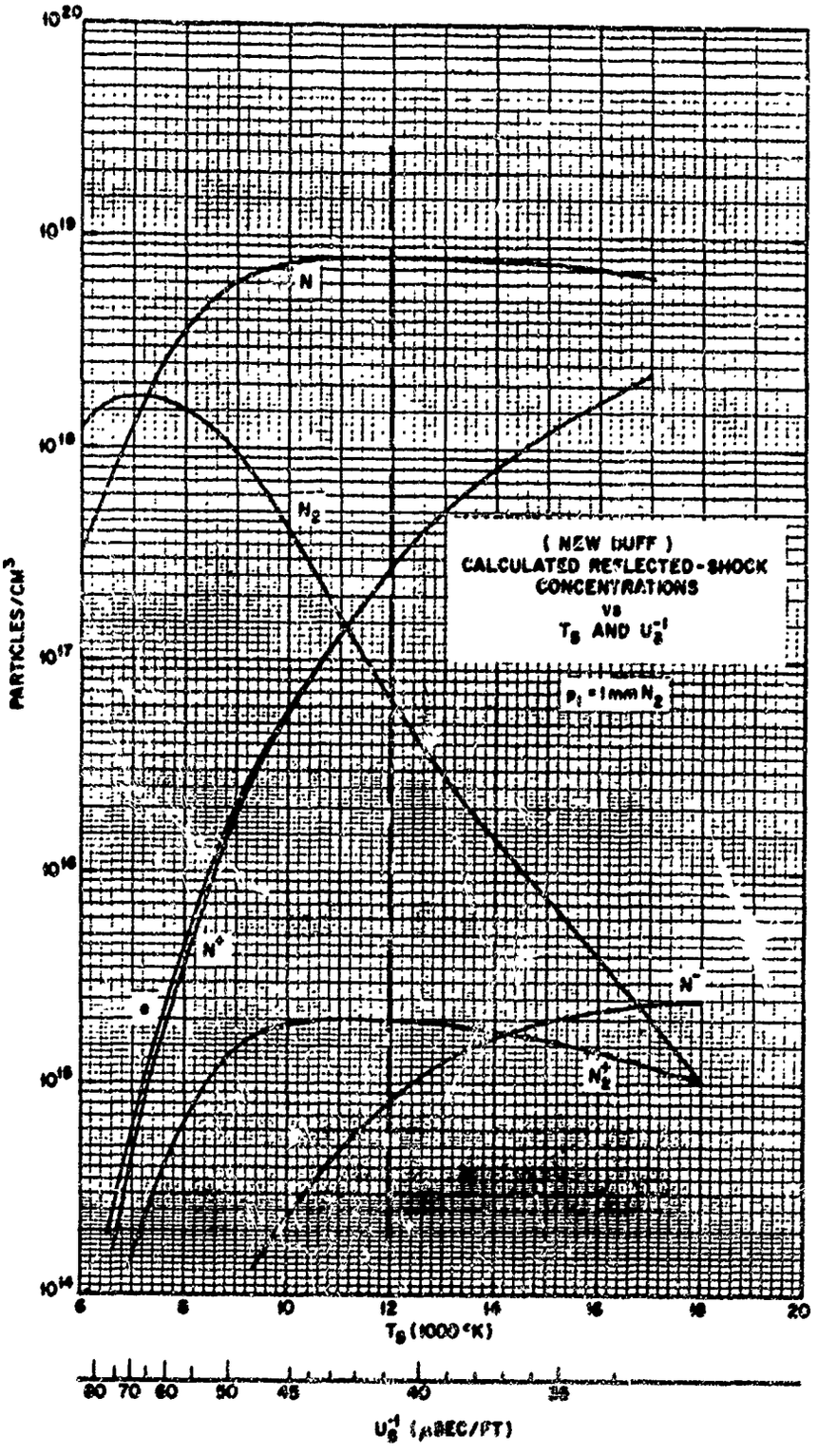

Fig. 16 Reflected Shock Concentrations Versus T_5 and U_s^{-1}, p_1 = 1 mm N_2 (New Duff)

Measurements of the N^+ and electron densities actually achieved in the reflected shocks were made using the time-resolved profiles of Hβ as recorded by the Gaertner drum spectrograph, Fig. 4. The theory of Griem-Kolb-Shen (Ref. 29) was used to interpret the Hβ line widths in terms of ion density. One percent diluent of hydrogen was added to the nitrogen by having Matheson Company prepare the N_2 plus 1 percent H_2 mixture in large cylinders. The temperatures T_5 inferred from the measured ion densities agreed to within 250 K° in 10,000°K with those determined from the measured reciprocal incident shock velocities U_s^{-1}, Fig. 16. Previous ion density measurements (Ref. 4) on 20 shots for this range of shock conditions showed that the calculated equilibrium ion densities, Fig. 16, were actually achieved in the reflected shock gas samples, and, furthermore, that ionization equilibrium across the reflected shock front was achieved within the time resolution of the spectrograph of about 3 microseconds.

These results are of importance in the interpretation of the nitrogen continuum intensities reported here, since the product of the N^+ and e densities has been used to compute the free-free continuum intensity for the electron in the field of the positive ion (Karzas and Latter theory, Ref. 18) and the nitrogen recombination cross sections deduced from the continuum measurements also depend on the product of the ion and electron densities.

c. Experimental Measurements of Nitrogen Line-Plus-Continuum Radiation

The wavelengths of the first four photomultiplier bandpasses listed in Table 2 were chosen so that on-band-off-band technique of absolute intensity measurements could be applied to the $N_2(2+)$ 3371 Å (0,0) band head and to the $N_2^+(1-)$ 3914 Å (0,0) band head in order to compare the relative contributions of these two systems for the same thermodynamic conditions, as well as to check on the validity of the f-values for these two systems presently used in the SACHA code, Table 1. The wavelengths of the other five bandpasses cover the range from 4700 Å to 6000 Å where the $N_2(1+)$ bands are expected by the SACHA calculations, Table 4 and Fig. 15, to make contributions of comparable magnitude to the $N_2^+(1-)$ bands. Our main objective in this experiment is to determine the shape and magnitude of the spectral continuum intensity underlying these extensive rotational-vibrational band systems. Our plan was to subtract the SACHA calculations of the average line contributions for a given shock condition from the measured total intensity to determine the continuum intensity. The nitrogen continuum processes aforementioned are expected to be on the threshold of making significant contributions to the spectral radiation at around 9000°K and above for the reflected shocks in pure nitrogen for p_1 = 1 mm starting pressure shown in Fig. 16. The reflected shock density is approximately constant at 0.124 ρ_o for the temperature range from 9000° to 12,000°K, Fig. 16. Of particular interest is the fact that the SACHA calculations of average line emissivity, Fig. 15, show a temperature-insensitive emissivity plateau for each bandpass beginning at around 10,000°K. We have used this plateau to advantage in an extensive set of measurements of the N_2^+ 3914 Å (0,0) band intensity (Refs. 3 and 4) and are continuing here to exploit it for simultaneous intensity measurements of all three molecular band systems of nitrogen. N_2 is dissociating very rapidly in this temperature region, Fig. 16, but the increasing temperature maintains the excited state populations at a more or less constant level. Figure 17 shows the measured absolute brightnesses B_N^λ in ergs sec^{-1} cm^{-2} $ster^{-1}$ (10 Å)$^{-1}$ for a 7.3 cm pathlength for eight shots into 1 mm N_2 downstream for the on-band-off-band wavelengths of 3371 Å (·) and 3425 Å (○),

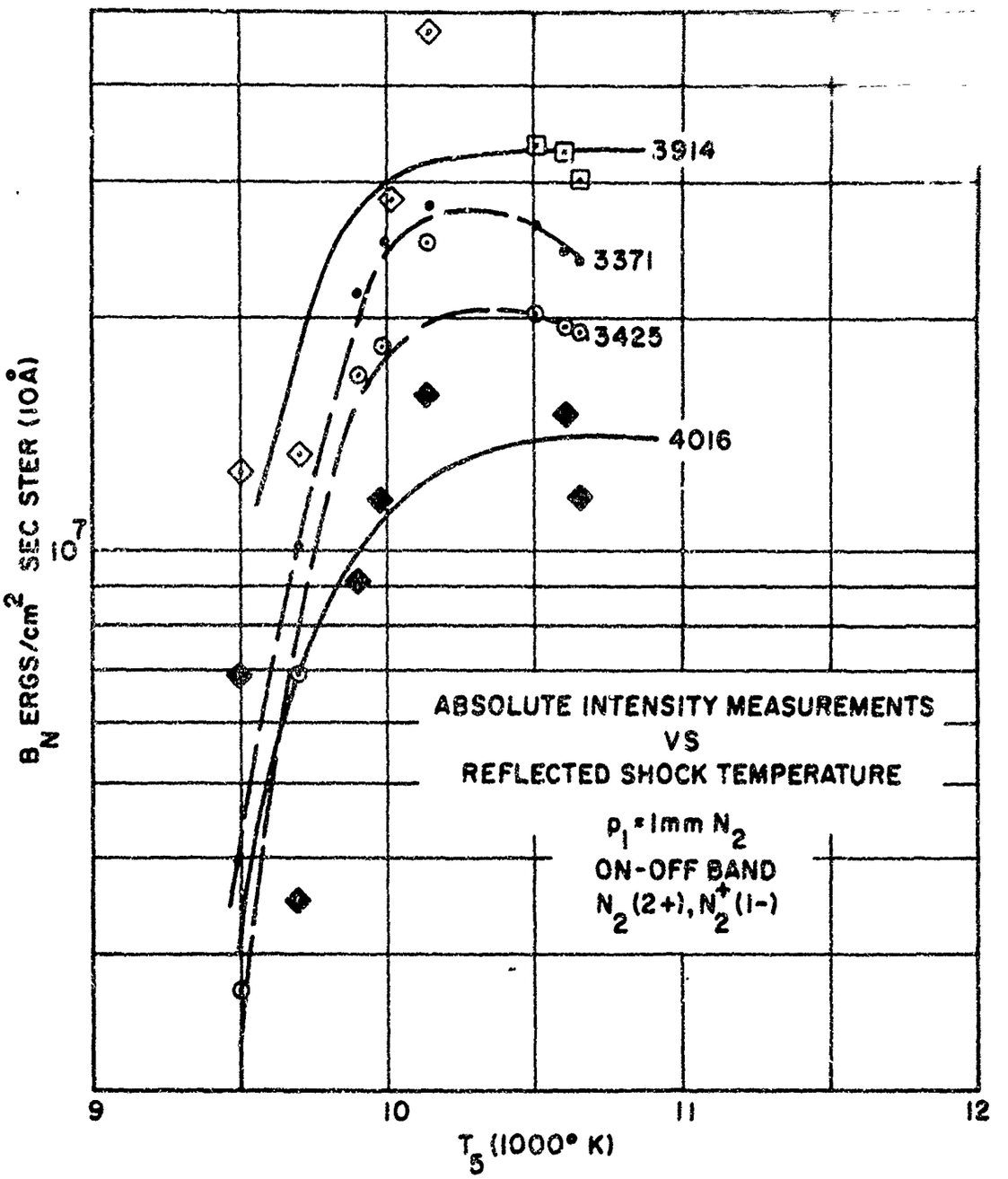

Fig. 17 Absolute Intensity Measurements of Nitrogen Line-Plus-Continuum Radiation versus T_5 for Wavelength Bandpasses 3371 Å, 3425 Å, 3914 Å, and 4016 Å

slashed curves, and of 3914 Å (□) and 4016 Å (■), solid curves. These brightnesses are the total measured line-plus-continuum brightnesses for these thermodynamic conditions in pure nitrogen, Fig. 16. Notice that a plateau is formed by the data at around 10,000°K in all four bandpasses which in general would indicate that the line contribution is dominating the structure of the emission, since the continuum intensity should increase monotonically with temperature. It should also be noted that the $N_2^+(1-)$ (0,0) radiation at 3914 Å exceeds that for the $N_2(2+)$ (0,0) band at 3371 Å for these shock conditions.

Figure 18 shows the measured total brightnesses per 7.3 cm pathlength for the five wavelength bandpasses in the $N_2(1+)$ radiating region. The curves are drawn as best fit curves to the experimental points. The important things to note about this array of experimental points are that no bandpass exhibits an outstandingly large intensity compared to the others, the magnitudes of the curves decrease with increasing wavelength, plateaus are also formed, and that these intensities are in general considerably lower than those for the $N_2^+(1-)$ and $N_2(2+)$ bandpasses, Fig. 17.

A look at the spectral emissivities for individual shots as derived from these data will point up these relations in magnitudes of the various band systems. Figure 19 shows the total measured emissivity per 7.3 cm pathlength for shot 477 for 9500°K and 0.125 ρ_o in nitrogen for which condition the continuum radiation is expected to be very small. The average emissivities predicted by the SACHA calculations for this condition taken from Fig. 15 are indicated by an "S" to the right of each SACHA point. The experimental on-band-off-band data for the $N_2(2+)$ 3371 Å (0,0) band are roughly one third that predicted by the SACHA code using the f-value of 0.07. If we follow our usual experimental practice of subtracting the off-band from the on-band emissivity for both the SACHA points and the data points in this case, the ratio of the experimental remainder to the SACHA remainder is indicative of a correction factor to the $N_2(2+)$ f-value of 0.07 presently used in the SACHA code. This correction factor for the $N_2(2+)$ for this shot is 2 ÷ 9 or 0.22.

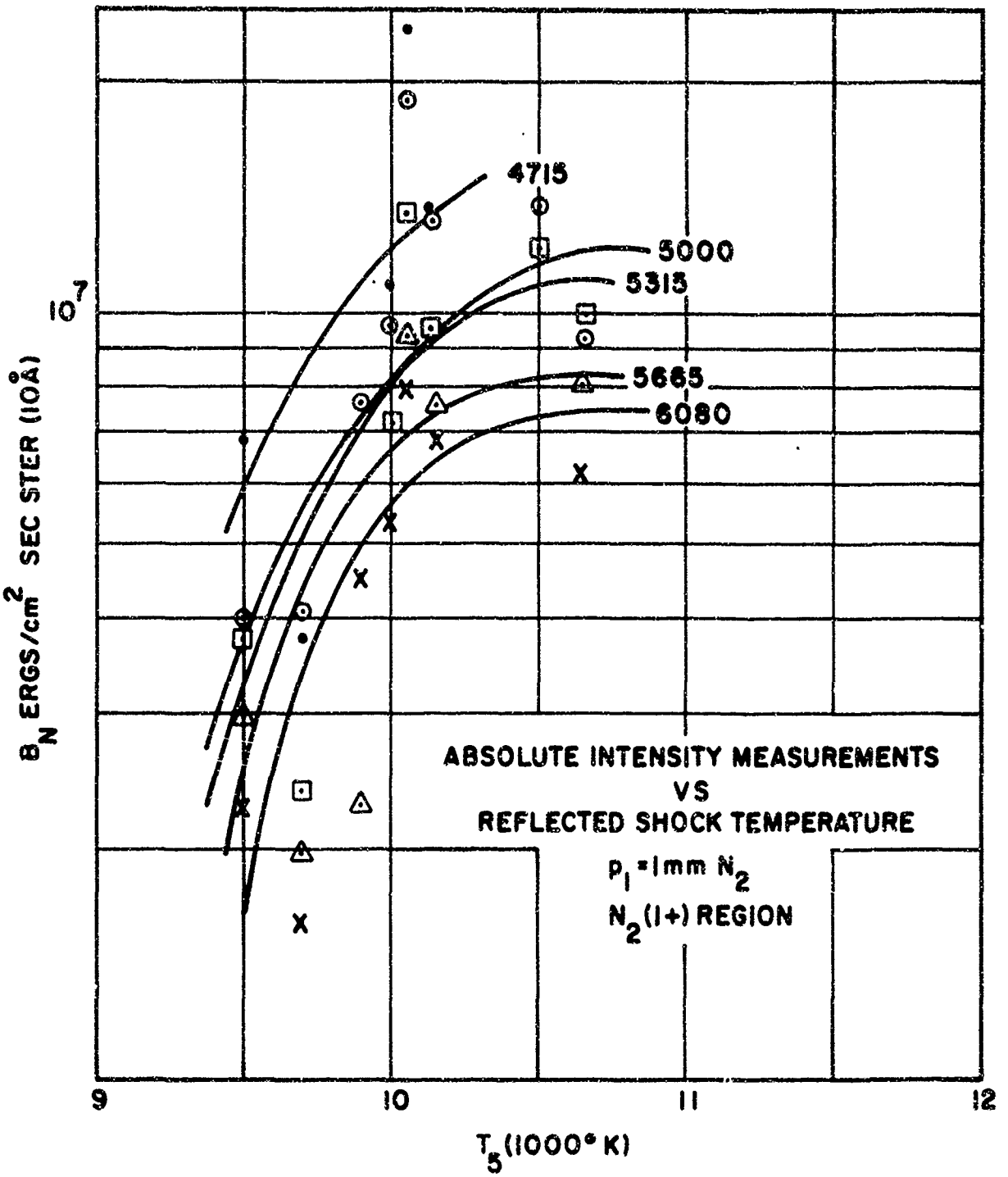

Fig. 18 Absolute Intensity Measurements of Nitrogen Line-Plus-Continuum Radiation versus T_5 for Five Wavelength Bandpasses between 4715 Å and 6050 Å

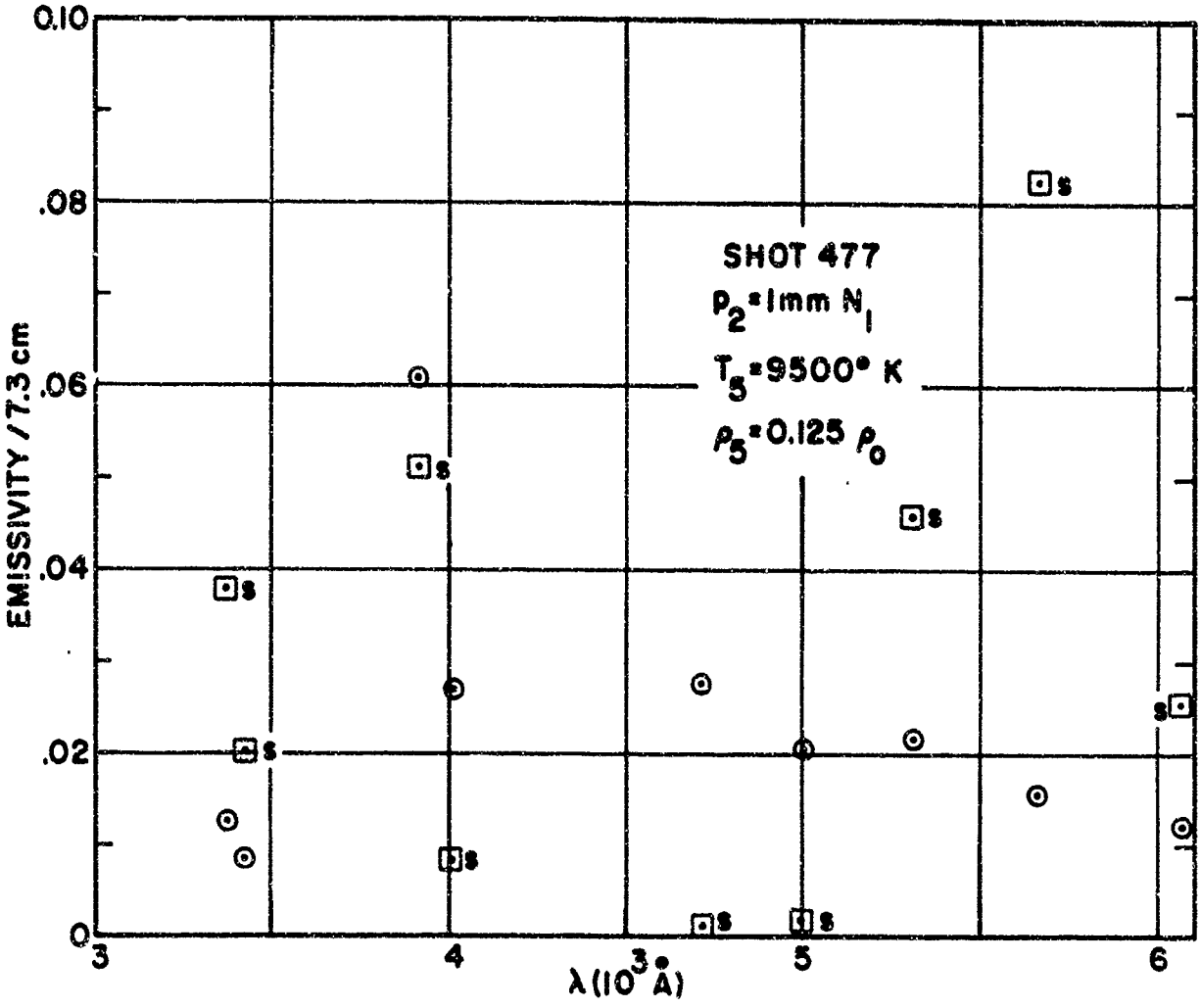

Fig. 19 Measured Total Spectral Emissivity per 7.3 cm Pathlength for Shock-Heated N2 at 9500°K and 0.125 ρ_0 versus SACHA Predictions for the Line Contribution

In the case of the $N_2^+(1-)$ system, Fig. 19, the magnitudes of the experimental emissivities for the on-band and for the off-band measurements exceed those predicted by the SACHA calculations for the rotational line contributions from all band systems for these two wavelengths (3914 Å and 4016 Å). However, the correction factor to the $N_2^+(1-)$ f-value of 0.0348 (Ref. 13) obtained by differencing is 0.80, which is within the error flag of the experimental data.

Similar comparisons for the $N_2(1+)$ bandpasses, Fig. 19, are somewhat confused because the general trend with wavelength of the experimental data points does not resemble that predicted by the SACHA calculations using the f-value of 0.02 for the $N_2(1+)$ transition. It is clear, however, that the f-value of 0.02 for this transition is too high since it predicts emissivities at 5330 Å and 5665 Å greater than those for the $N_2^+(1-)$ systems and this prediction is not borne out in general by the experimental data points, Fig. 19. At 4715 Å and 5000 Å, the reverse is true, i.e., the measured total emissivities exceed by a large factor the SACHA points, which could be due to an unwarranted cut off in vibrational transitions (v',v''), possibly in the SACHA code. The question of what band system or combination of band systems is contributing to form the experimental profile in this region, Fig. 19, remains unanswered. We tried to select the 4715 Å and 5000 Å bandpasses so that the wings of the Stark-broadened profile of Hβ (4861 Å) would not contribute in these bandpasses, and, indeed, we feel that the Hβ contributions to the intensities in this case are small because the ion density is relatively low ($N_{ion} = 3.5 \times 10^{16}$ cm^{-3}) in this case and the Hβ profile more "peaked." It is possible that the $\Delta v = 3$ sequence of the $N_2^+(1-)$ system, i.e., the 5228 Å (0,3), 5149 Å (1,4), 5077 Å (2,5) systems of N_2^+ are instrumental in filling in the shape under the experimental data points. We have been able to record this sequence on the time-resolved Gaertner drum spectra as well as the stronger $\Delta v = 2$ and $\Delta v = 1$ sequences, beginning with the 4709 Å (0,2) and the familiar 4278 Å (0,1) systems, respectively. If this is the case the Franck-Condon factors $q_{(v',v'')}$ for these $N_2^+(1-)_{(v',v'')}$ systems (Ref. 24) may be in error. It is pertinent to point out that we have not recorded

the $N_2(1+)$ systems in this 5000 Å to 5700 Å range with either the time resolved Gaertner spectrograph or with the high resolution Meinel. Whereas we have said that the $N_2^+(1-)$ $\Delta v = 3$ sequence, 5232 Å to shorter wavelengths, has been observed.

In view of these arguments we have selected the experimental and SACHA points at 5665 Å, Fig. 19, to obtain leverage on the $N_2(1+)$ f-value. For this shot a correction factor of 0.2 to the $N_2(1+)$ f-value of 0.02 is indicated, i.e., the $N_2(1+)$ f-value obtained from this analysis is 0.04 for this set of data.

The lower graph in Fig. 20 shows the measured spectral emissivities for the reflected-shock condition in pure N_2 of 10,500°K and 0.124 ρ_o for which condition the continuum radiation is expected to contribute. Our original thinking based on measured intensities (Ref. 3) was to the effect that the continuum radiation was making the major contribution to the emission in the 4730 Å to 5500 Å range for this condition. In view of the just previous discussion it may very well be that the $N_2^+(1-)$ radiation dominates the emission for this condition which point is also borne out by the plateau temperature dependence shown in the experimental intensity data, Fig. 18. The experimental data points in Fig. 20 are the average of the numbers for two shots, shots 468 and 470. For these shots the ion density of 8.0×10^{16} cm^{-3} as determined by the analysis of the time-resolved Stark-broadened Hβ profile indicated shock temperatures of 10,650°K for both shots as compared to temperature of 10,500°K determined from the measured shock velocities for both these shots. With this remarkable agreement in temperature as determined from two different techniques and in view of the fact that the ion density of 8.0×10^{16} cm^{-3} was actually measured by a very sensitive technique (Ref. 29), the experimental emissivities plotted in Fig. 20 represent our best effort to determine the line-plus-continuum radiation for this condition, regardless of how we may try in the following discussion to separate the line and the continuum contributions.

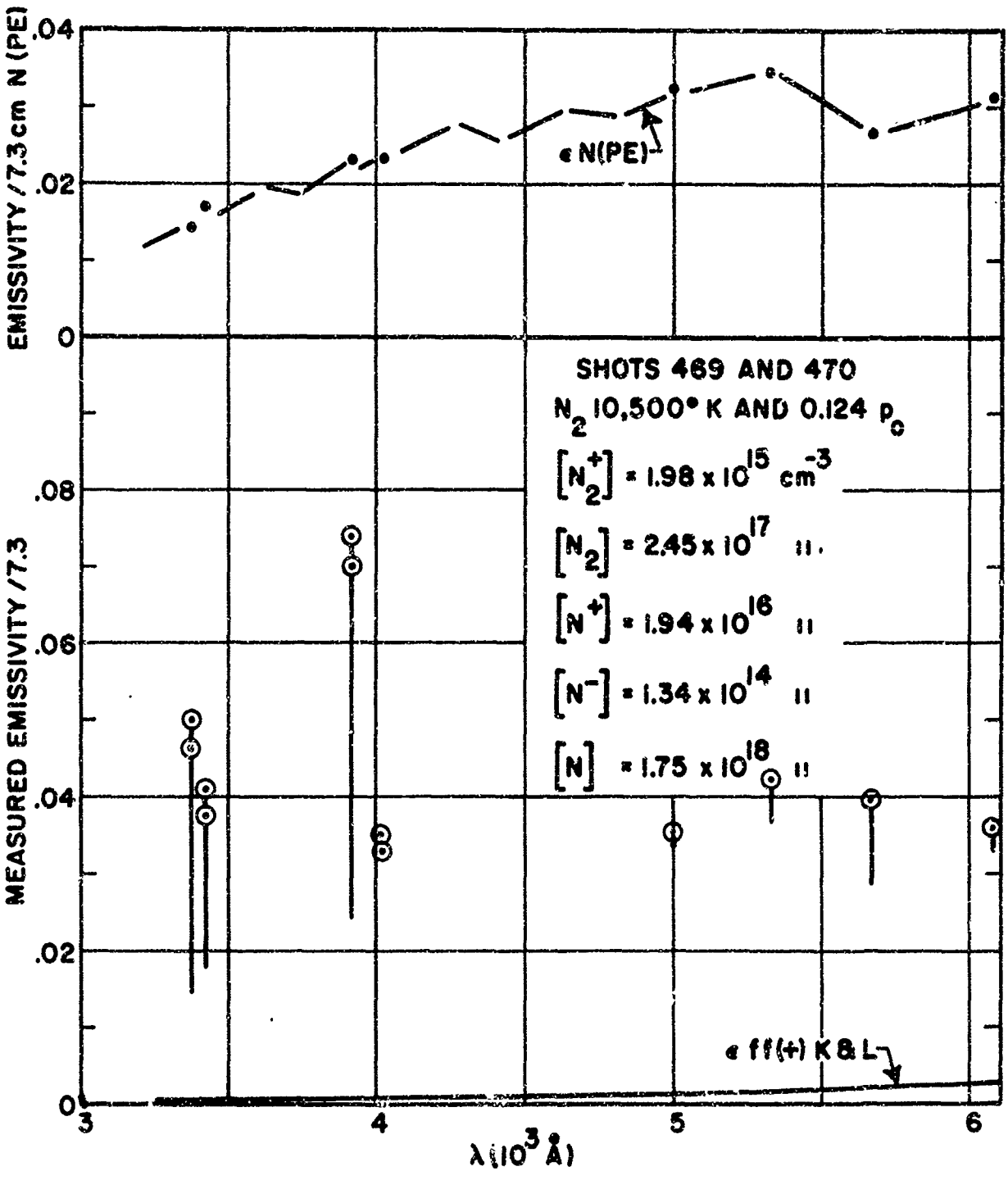

Fig. 20 Measured Emissivity per 7.3 cm Pathlength for Lines-Plus-Continuum for Shock-Heated N_2 at 10,500°K and 0.124 ρ_0 showing Continuum Emissivity Attributed to the Nitrogen Continuum Processes

The magnitudes of the SACHA average-line contributions are indicated by the bar graphs in Fig. 20 extending from the experimental points (o) downward. We have taken the liberty of reducing the SACHA $N_2(1+)$ emissivities by a factor of 0.2. The free-free contribution $\epsilon_{ff(+)}$ of the electron in the field of the positive ion (Ref. 18) is plotted on the curve near the abscissa. The difference in emissivity between this lower $\epsilon_{ff(+)}$ curve and the bottom of the SACHA bar graphs supposedly represents the magnitudes of the spectral continuum radiation. These differences are shown in Fig. 20 in the upper plot. The skeleton curve was put in to indicate the shape of the nitrogen recombination cross section since $\epsilon_\lambda = \sigma^\lambda_{N(PE)}[N](7.3\ cm)$. The general shape of this curve is reasonable for such a process since an increasing number of excited states contribute to the radiation going to lower photon energies or longer wavelengths. Using these emissivities, upper curve Fig. 20, we have computed the nitrogen recombination cross sections for each wavelength for 10,500°K, and these vary in magnitude with the emissivity (upper curve Fig. 20) from the absolute values of 2.6×10^{-22} cm^2 to 6.2×10^{-22} cm^2 between 3371 Å and 6050 Å.

The N^- photodetachment cross sections determined by Boldt (Ref. 12) would predict emissivities for the shock conditions of Fig. 20 of 0.12 at 4300 Å to 0.08 at 6100 Å. It is clear that we do not find emissivities of this magnitude in our data, upper and lower curves, Fig. 20. If all the emissivity in the upper curve Fig. 20 were used to compute an N^- photodetachment cross section our values would be 2.5×10^{-17} cm^2 at 4300 Å and 5.8×10^{-17} cm^2 at 6100 Å, which compare with Boldt's values of 1.14×10^{-16} cm^2 at 4300 and 0.83×10^{-16} cm^2 at 6100 Å. Both sets of data employed an electron affinity of 1.1 eV for atomic nitrogen. We have assumed no contribution from the N^- photodetachment process in our reported values of the N recombination cross sections for 10,500°K of 2.6×10^{-22} cm^2 to 6.2×10^{-22} cm^2 for the visible region.

d. Discussion of Nitrogen Lines-Plus-Continuum Measurements

The average of the correction factors to the $N_2(2+)$ and the $N_2^+(1-)$ f-values presently used by the SACHA code, Table 1, as obtained from our on-band, off-band intensity measurements for eight shots are 0.6 for the $N_2(2+)$ transition and 1.14 for the $N_2^+(1-)$ transition. Our values for the f-values, then, are 0.042 for the $N_2(2+)$ and 0.040 for the $N_2^+(1-)$ system. Reduction of the f-value of 0.02 for the $N_2(1+)$ transition to 0.003 gave a more reasonable shape to the spectral emissivity for the nitrogen photoelectric process for 10,500°K and 0.124 ρ_o, and this lower value predicted line intensities more in keeping with our measured intensity for lower temperatures. There seems to be some doubt raised by these SACHA experimental comparisons as to the general shape of either the $N_2^+(1-)$ intensity envelope or the $N_2(1+)$ intensity envelope in the wavelength region of 4700 Å to 5700 Å.

The nitrogen continuum radiation begins to make appreciable contribution for the temperature range of 9000°K to 11,000°K and one-eighth normal density, with the nitrogen recombination process being the main contributor. The N^- photodetachment cross sections of $\approx 10^{-16}$ cm^2 reported by Boldt predict much larger intensities in the visible region than we have found in our intensity measurements of lines plus all continuua, leaving it still an open question as to whether the negative nitrogen ion is actually formed.

7. ATTEMPTS TO OBSERVE THE O^- PHOTOELECTRIC EDGES

The electron affinity of atomic oxygen is 1.46 eV as determined by Branscomb, et al. (Ref. 30), and represents the energy difference of the ground state of O^- below the ground state (^3P) of O. This in effect makes the $^1D_2$ and $^1S_0$ states of atomic oxygen at energies above the O^- ground state of 3.43 eV and 5.64 eV, respectively, corresponding to the wavelengths of 3600 Å and 2200 Å. At these wavelengths or photon energies one might reasonably expect to see photoelectric edges for O^- due to the photon detachment of an electron from O^- via one of these states or from the inverse process, i.e., the attachment of an electron of zero energy to the oxygen atom into the ^1D or ^1S states and the emission of a photon of either 3.43 eV or 5.4 eV energy.

All efforts to observe these O^- photoelectric edges in the equilibrium radiation from shock-heated oxygen have met with little or no success in the past (Refs. 3 and 4). In the range of conditions where the O^- photodetachment process should be the dominant continuum process, between 7000°K and 9000°K at about one-third normal density, the O_2(S-R) discrete emission spectrum has dominated the spectra in the wavelength region of the predicted edges.

a. Addition of Li_2O Into Shocks in Oxygen

In view of this we have tried to enhance the continuum due to O^- by adding small amounts of Li_2O into shocks with p_1 = 3 mm O_2. It was hoped that the low ionization energy (5.4 eV) of atomic lithium, Li, would provide at lower temperatures sufficient electrons for O attachment processes such that it would be possible to observe an intensity variation under the O_2(S-R) lines at around 3600 Å which we could attribute to the O^- photodetachment process.

Accordingly, Li_2O in amounts varying from 1 mg to 0.05 mg ground into paper were hung in the shock tube 6 inches from the reflector plate, and shock waves initiated into starting pressures downstream of p_1 = 3 mm O_2. No discontinuous variation in the intensity envelope under the observed O_2(S-R) spectrum was observed nor was there any observed change in the

slope from what had normally been seen in shocks in pure O_2. It is reasonably clear from the observed Stark-broadened LiI lines at 4958 Å and 4603 Å that the Li_2O molecules did indeed break up and form Li atoms and ions in sufficient quantities to enhance the O^- continuum intensity. However, we found ourselves at a loss without a lengthier development of diagnostic techniques to ascribe a temperature to the reflected shock gas samples. From black body intensity considerations it is possible that for the temperature range which we estimated to be from 6000°K to 9000°K, that a change in slope, had it been observed, could be due to a shift in the wavelength of peak black body intensity, rather than due to an edge of the O^- photodetachment continuum. Hence, any results we might have gotten would have been inconclusive as regards O^-.

b. Determination of O^- Continuum Intensity from Experimental-SACHA Analysis of O_2 S-R Line Shapes

A technique has been developed for the detection and determination of the absolute magnitude for the spectral continuum intensity underlying a blanket of rotational lines. We have applied it to oxygen shock spectra for the condition of 8400°K and 0.33 ρ_o discussed previously in connection with the O_2(S-R) rotational line shape study. For this condition a continuum underlying the O_2(S-R) rotational lines attributable to the O^- photodetachment process has been ascertained and an absolute emissivity of 0.032 at 3400 Å for the O^- continuum determined from the analysis of the shape of the clump of lines at this wavelength Sec. 5c, Fig. 14. This emissivity is more than twice the value of 0.013 predicted by Branscomb's cross sections for the wavelength region of 4000 Å to 5000 Å for this shock condition. These results are indicative of a photoelectric edge in O^- between 4000 Å and 3400 Å. Even though our findings are of a preliminary nature in view of the uncertainties in frequency positions of the O_2(S-R) lines (Sec. 5c), the technique warrants discussion in that by its extension to the study of lines at other wavelengths it will be possible to actually map out the shape of the spectral continuum.

The determination of the absolute emissivity of the continuum required the following things: SACHA calculation of the absolute emissivity of the detailed rotational intensity envelope for the lines only, and an experimental relative intensity envelope for lines plus continuum determined from photometry of a portion of the Meinel shock spectrum. For the 8400°K oxygen condition in point, normalization of the experimental relative intensity envelope to the SACHA envelope for the peak of the clump of lines at 3400 Å labeled (0,14) R 27 P 23, Fig. 14, gave the initial results shown in Fig. 21. The fact that the experimental envelope did not come close to fitting the SACHA envelope but was in general considerably higher in the valleys, is indicative of the presence of an underlying continuum in the experimental data. The amount of the experimental curve which has to be subtracted in order to obtain a peak-to-minimum fit with the SACHA line structure can be converted to an absolute emissivity for the continuum at this wavelength, since we know the absolute excursion in emissivity for the SACHA line structure. Once this amount has been subtracted from the experimental relative intensity points the experimental curve is then normalized a second time to the SACHA curve with the results shown in Fig. 14. The general fit in the structure of the SACHA line clump (dotted curve) labeled (0,14) R (27) P (23) with the experimental shape (solid curve) lends added weight to the validity of such a technique in the determination of the O^- continuum emissivity of 0.032 under this line grouping. The accuracy of the absolute magnitude of this emissivity is dependent on the validity of f-value of 0.0348 (Ref. 6) for the $O_2(S\text{-}R)$ transition and on the line width and frequency positions used in the SACHA calculations.

The relation of this value of the O^- continuum emissivity to the spectral emissivity predicted by Branscomb's O^- photodetachment cross sections for this shock condition is shown in Fig. 22. The solid portion of the curve extending from 8400 Å (1.46 eV) to 4500 Å shows the extent in energy of Branscomb's work and the remaining dotted portion shows the prediction of the discontinuous increase in the O^- cross section at 3600 Å and 2400 Å due respectively to the ^1D and ^1S states of atomic oxygen.

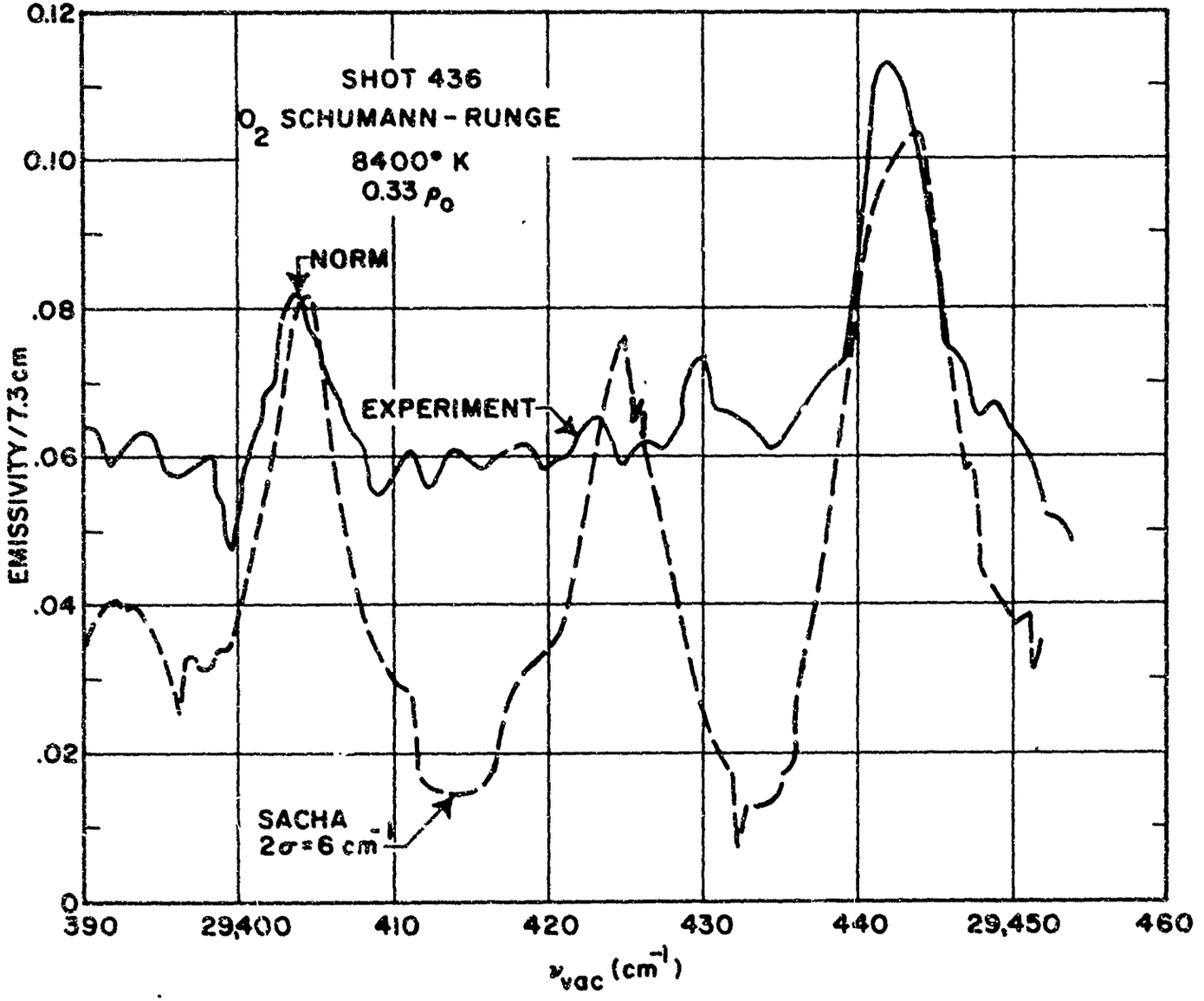

Fig. 21 Normalization of Relative Spectral Intensity Curve (Solid) from Photometry of Meinel O_2 at 8400°K to the SACHA Calculation of Spectral Emissivity Showing the Effects of the O^- Continuum Radiation in the Failure to Fit

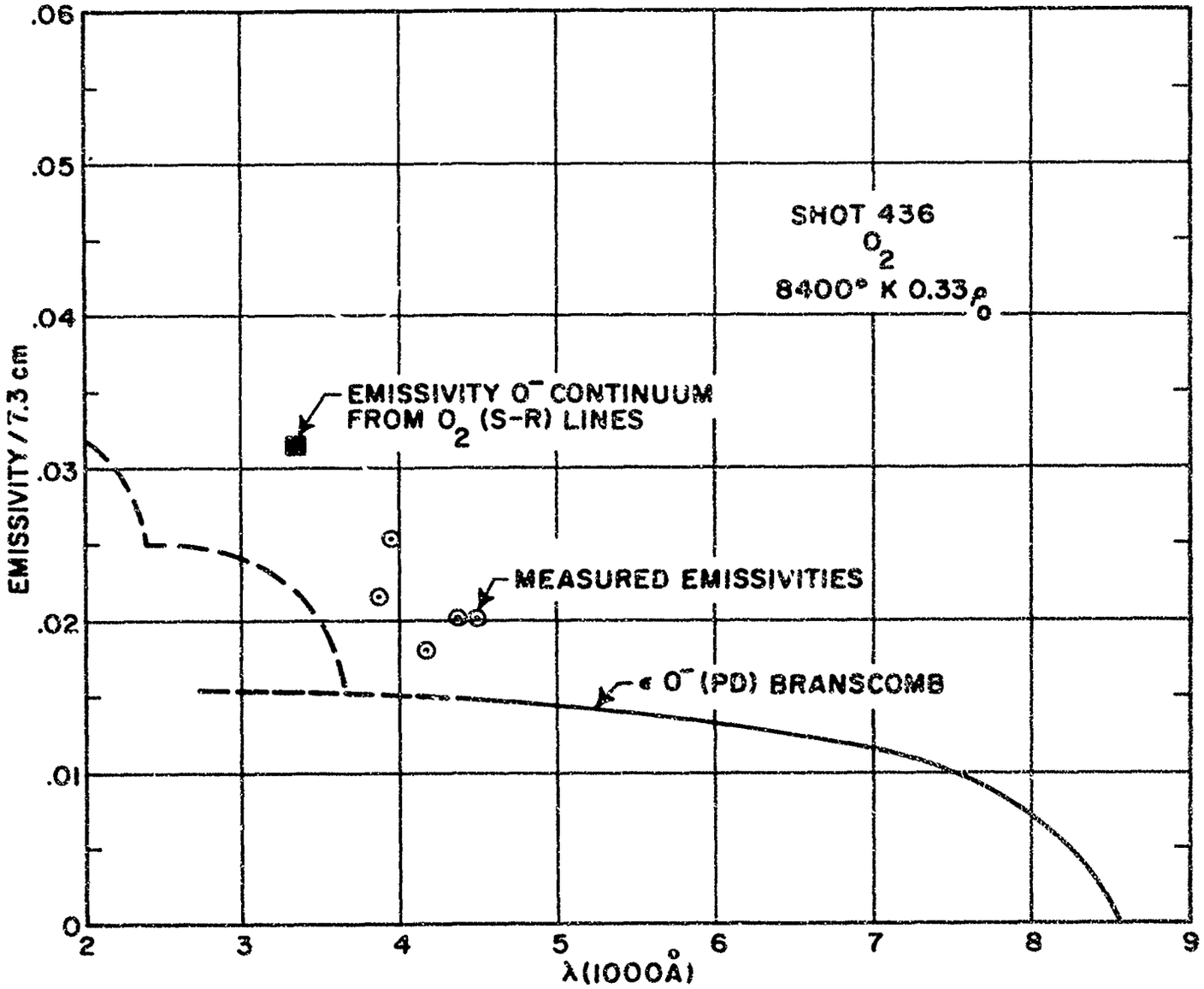

Fig. 22 Evidence of O^- Photoelectric Edge at 3600 Å from O_2 (S-R) Rotational Line-Shape Analysis for O_2 at 8400°K and 0.33 ρ_o

The value of 0.032 obtained from the line shape analysis (✱) is shown at 3400 Å, and the experimentally measured absolute intensities at 3890 Å, 3947 Å, 4368 Å and 4500 Å from photomultiplier measurements of absolute intensity for this shot are shown also (⊖). None of the experimental points exceeds 0.023 and a portion of the measured average emissivities must of necessity be due to O_2(S-R) lines, which when subtracted would bring the total measured points for continuum contribution only closer to the Branscomb curve. Thus we have the first quantitative observation of an O^- continuum for high-temperature shock-heated oxygen, which confirms Branscomb's cross sections for the O^- photodetachment process as well as gives evidence of an O^- photoelectric edge (^1D) between 3900 Å and 3400 Å.

REFERENCES

1. Meyerott, R. E., J. Sokoloff and R. W. Nicholls, Mean Absorption Coefficients of High Temperature Air, Lockheed LMSC 288052, Sept. 1959
2. Armstrong, B. H., Mean Absorption Coefficients of Air, Nitrogen and Oxygen from 22,000° to 220,000°, LMSD 49759, 1959
3. Armstrong, B. H., D. H. Holland and R. E. Meyerott, Absorption Coefficients of Air from 22,000° to 220,000°, AFSWC TR 58-36, 1958
4. Buttrey, D. E. and J. B. Gibson, Radiative Properties of High Temperature Oxygen and Nitrogen, AFSWC RTD-TDR 63-3047, June 1963
5. Armstrong, B. H., D. E. Buttrey, L. Sartori, A. J. F. Siegert and J. D. Weisner, Radiative Properties of High Temperature Gases, AFSWC TR 61-72, Oct. 1961
6. Treanor, C. E. and W. H. Wurster, Measured Radiation Probabilities for the Schumann-Runge System of Oxygen, J. Chem. Phys., Vol. 32, 1960
7. Keck, J., Camm, B. Kivel and T. Wentink, Ann. Phys., Vol. 7, 1, 1959
8. Weber, D. and S. S. Penner, Absolute Intensities for the Ultraviolet γ Bands of NO, J. Chem. Phys., Vol. 26, pp 860-861, 1937
9. Bethke, G., J. Chem. Phys., Vol. 31, 662, 1959
10. Bethke, G., J. Chem. Phys., Vol. 31, 669, 1959
11. Boldt, G., Z. Physik, Vol. 154, p. 319, 1959
12. Boldt, G., Z. Physik, Vol. 154, p. 330-338, 1959
13. Bennett, R. C. and F. W. Dalby, J. Chem. Phys., Vol. 31, p. 434, 1959
14. Churchill, D. R., S. A. Hagstrom and R. K. M. Landshoff, The Spectral Absorption Coefficient of Heated Air, J. Quant. Spectrosc. Radiat. Transfer, Vol. 4, pp. 291-321, 1964
15. Breene, R. G. and M. C. Nardone, Radiant Emission from High Temperature Air, J. Quant. Spectrosc. Radiat. Transfer, Vol. 2, p. 273-292, 1962
16. Harrington, J. D., An f/3.5 Medium Dispersion Spectrograph, Naval Research Laboratory, USNRL Report 5446, 1960

17. Krindach, N. I., N. N. Sobelev and L. N. Trinitski, Optics and Spectroscopy, Vol. 15, p. 326, 1963

18. Karzas, W. J. and R. Latter, Astrophys. J., Suppl. No. 55, Vol. 6, p. 167-212, 1961

19. Chen, Shang-yi and Makato Takeo, Rev. Mod. Phys., Vol. 29, p. 20, 1957

20. Breene, R. G., Rev. Mod. Phys. Vol. 29, p. 94, 1957

21. Margenau, H. and M. Lewis, Rev. Mod. Phys., Vol. 31, p. 569, 1959

22. Baranger, M., Spectral Line Broadening in Plasmas in Atomic and Molecular Processes, edited by D. R. Bates, Academic Press, New York, 1962

23. Nicholls, R. W., The Franck-Condon Factor $q(v',v'')$ Array to High Vibrational Quantum Numbers for the O_2 ($B^3\Sigma^-$ - $X^3\Sigma_g^+$) Schumann-Runge Band System, Can. J. Phys., Vol. 38, p. 1705, 1960

24. Nicholls, R. W., Franck-Condon Factors to High Vibrational Quantum Numbers: N_2 and N_2^+, J. Res. N.B.S., Vol. 65A, p. 451, 1961

25. Nicholls, R. W., Franck-Condon Factors to High Vibrational Quantum Numbers II: SiO, MgO, AlO VO, NO, J. Res. N.B.S., Vol. 66A, p. 227, 1962

26. Childs, W. H. J., Proc. Roy. Soc. (London), Vol. 37, p. 641, 1932

27. Lochte-Holtgreven, V. W. and G. H. Dieke, Ann. Physik, Vol. 3, p. 937, 1929

28. Kramers, H. A., Phil. Mag., Vol. 46, p. 836, 1923

29. Griem, H. R., A. C. Kolb, K. Y. Shen, Stark Broadening of Hydrogen Lines in a Plasma, Phys. Rev., Vol. 116, p. 4-10, 1959

30. Branscomb, L. A., D. S. Burch, S. J. Smith and S. Geltman, Photodetachment Cross Section and the Electron Affinity of Atomic Oxygen, Phys. Rev., Vol. 111, p. 504-513, 1958

DISTRIBUTION

No. cys

HEADQUARTERS USAF

Hq USAF, Wash, DC 20330

1 (AFRNE-B, Maj Lowry)

1 (AFTAC)

1 USAF Dep, The Inspector General (AFIDI), Norton AFB, Calif 92409

1 USAF Directorate of Nuclear Safety (AFINS), Kirtland AFB, NM 87117

MAJOR AIR COMMANDS

1 AFSC (SCT), Andrews AFB, Wash, DC 20331

1 AUL, Maxwell AFB, Ala 36112

2 USAFIT, Wright-Patterson AFB, Ohio 45433

AFSC ORGANIZATIONS

1 AFSC Scientific and Technical Liaison Office, Research and Technology Division, AFUPO, Los Angeles, Calif 90045

1 FTD (TDBTL), Wright-Patterson AFB, Ohio 45433

1 AF Materials Laboratory, Wright-Patterson AFB, Ohio 45433

1 AF Flight Dynamics Laboratory, ATTN: Mr. F. D. Adams, Wright-Patterson AFB, Ohio 45433

1 RTD, Bolling AFB, Wash, DC 20332

1 ESD (ESTI, L. G. Hanscom Fld, Bedford, Mass 01731

1 RADC (EMLAL-1), Griffiss AFB, NY 13442

KIRTLAND AFB ORGANIZATIONS

1 AFSWC (SWEH), Kirtland AFB, NM 87117

AFWL, Kirtland AFB, NM 87117

20 (WLIL)

1 (WLA)

1 (WLAV)

1 (WLR)

1 (WLRM)

5 (WLRT)

1 (WLRTH, Lt DeBord)

OTHER AIR FORCE AGENCIES

1 SAAMA (SAW), Directorate of Special Weapons, Kelly AFB, Tex 78241

1 AFOSR (SRGL, Bldg T-D, Wash, DC 20333

UNCLASSIFIED

Security Classification

DOCUMENT CONTROL DATA - R&D

(Security classification of title, body of abstract and indexing annotation must be entered when the overall report is classified)

1. ORIGINATING ACTIVITY *(Corporate author)*

Lockheed Missile and Space Company
3251 Hanover Street
Sunnyvale, California

2a. REPORT SECURITY CLASSIFICATION

UNCLASSIFIED

2b. GROUP

3. REPORT TITLE

OPACITY OF LOW TEMPERATURE AIR

4. DESCRIPTIVE NOTES *(Type of report and inclusive dates)*

July 1, 1964-July 1, 1965

5. AUTHOR(S) *(Last name, first name, initial)*

Buttrey, D. E.; McChesney, H. R.

6. REPORT DATE	7a. TOTAL NO. OF PAGES	7b. NO. OF REFS
November 1965	90	30

8a. CONTRACT OR GRANT NO.	AF 29(601)-6433	9a. ORIGINATOR'S REPORT NUMBER(S)	
b. PROJECT NO.	5710	AFWL-TR-65-134	
c. Subtask No.	07.003	9b. OTHER REPORT NO(S) *(Any other numbers that may be assigned this report)*	
d.			

10. AVAILABILITY/LIMITATION NOTICES

This document is subject to special export controls and each transmittal to foreign governments or foreign nationals may be made only with prior approval of AFWL (WLRT), Kirtland AFB, NMex, 87117. Distribution is controlled to protect

11. SUPPLEMENTARY NOTES

technical knowledge which has advanced the state of the art.

12. SPONSORING MILITARY ACTIVITY

AFWL (WLRT)
Kirtland AFB, NM 87117

13. ABSTRACT

Emission spectrograms with 0.2 Angstrom resolution have been recorded for shock-heated air, oxygen, nitrogen, and nitrous oxide for temperatures from 6,000 to 12,000 degrees Kelvin and densities from 0.1 to 3.3 normal. The beta and gamma band systems of nitrous oxide were not observed in these spectra, leading to the conclusion that Bethke's f-values are at least a factor of two too high. A SACHA peak-to-minimum fit to the experimental profile of singly ionized molecular nitrogen 3,914 Angstrom band head was found for a Lorentz line width of 1.9 per centimeters for the condition of 9,500 degrees Kelvin and 0.125 normal density in pure nitrogen. An upper limit for the molecular oxygen-atomic oxygen collision cross section of less than or equal to 2×10^{-14} square centimeters has been obtained from analysis of oxygen Schumann-Runge emission lines for the condition of 8,400 degrees Kelvin and 0.3 normal density. Absolute intensity measurements of nitrogen continuum radiation in the molecular regime below 12,000 degrees Kelvin have failed to show the intensity predicted by Boldt's negatively charged atomic nitrogen photodetachment cross section. The addition of lithium oxide to shocks in oxygen has failed to show any real evidence of the negatively charged atomic oxygen photoelectric edge at 3,600 Angstroms. However, SACHA experimental analyses of the oxygen Schumann-Runge rotational lines at 3,400 Angstroms has yielded some quantitative evidence of the existence of an edge underlying the molecular oxygen rotational line.

DD FORM 1 JAN 64 1473

UNCLASSIFIED

Security Classification

14. KEY WORDS	LINK A		LINK B		LINK C	
	ROLE	WT	ROLE	WT	ROLE	WT
Low-temperature air Opacities SACHA calculations Line widths Collision cross sections Emission studies						

INSTRUCTIONS

1. ORIGINATING ACTIVITY: Enter the name and address of the contractor, subcontractor, grantee, Department of Defense activity or other organization *(corporate author)* issuing the report.

2a. REPORT SECURITY CLASSIFICATION: Enter the overall security classification of the report. Indicate whether "Restricted Data" is included. Marking is to be in accordance with appropriate security regulations.

2b. GROUP: Automatic downgrading is specified in DoD Directive 5200.10 and Armed Forces Industrial Manual. Enter the group number. Also, when applicable, show that optional markings have been used for Group 3 and Group 4 as authorized.

3. REPORT TITLE: Enter the complete report title in all capital letters. Titles in all cases should be unclassified. If a meaningful title cannot be selected without classification, show title classification in all capitals in parenthesis immediately following the title.

4. DESCRIPTIVE NOTES: If appropriate, enter the type of report, e.g., interim, progress, summary, annual, or final. Give the inclusive dates when a specific reporting period is covered.

5. AUTHOR(S): Enter the name(s) of author(s) as shown on or in the report. Enter last name, first name, middle initial. If military, show rank and branch of service. The name of the principal author is an absolute minimum requirement.

6. REPORT DATE: Enter the date of the report as day, month, year, or month, year. If more than one date appears on the report, use date of publication.

7a. TOTAL NUMBER OF PAGES: The total page count should follow normal pagination procedures, i.e., enter the number of pages containing information.

7b. NUMBER OF REFERENCES: Enter the total number of references cited in the report.

8a. CONTRACT OR GRANT NUMBER: If appropriate, enter the applicable number of the contract or grant under which the report was written.

8b, &c, & 8d. PROJECT NUMBER: Enter the appropriate military department identification, such as project number, subproject number, system numbers, task number, etc.

9a. ORIGINATOR'S REPORT NUMBER(S): Enter the official report number by which the document will be identified and controlled by the originating activity. This number must be unique to this report.

9b. OTHER REPORT NUMBER(S): If the report has been assigned any other report numbers *(either by the originator or by the sponsor)*, also enter this number(s).

10. AVAILABILITY/LIMITATION NOTICES: Enter any limitations on further dissemination of the report, other than those imposed by security classification, using standard statements such as:

(1) "Qualified requesters may obtain copies of this report from DDC."

(2) "Foreign announcement and dissemination of this report by DDC is not authorized."

(3) "U. S. Government agencies may obtain copies of this report directly from DDC. Other qualified DDC users shall request through

_____."

(4) "U. S. military agencies may obtain copies of this report directly from DDC. Other qualified users shall request through

_____."

(5) "All distribution of this report is controlled. Qualified DDC users shall request through

_____."

If the report has been furnished to the Office of Technical Services, Department of Commerce, for sale to the public, indicate this fact and enter the price, if known.

11. SUPPLEMENTARY NOTES: Use for additional explanatory notes.

12. SPONSORING MILITARY ACTIVITY: Enter the name of the departmental project office or laboratory sponsoring *(paying for)* the research and development. Include address.

13. ABSTRACT: Enter an abstract giving a brief and factual summary of the document indicative of the report, even though it may also appear elsewhere in the body of the technical report. If additional space is required, a continuation sheet shall be attached.

It is highly desirable that the abstract of classified reports be unclassified. Each paragraph of the abstract shall end with an indication of the military security classification of the information in the paragraph, represented as *(TS), (S), (C), or (U)*

There is no limitation on the length of the abstract. However, the suggested length is from 150 to 225 words.

14. KEY WORDS: Key words are technically meaningful terms or short phrases that characterize a report and may be used as index entries for cataloging the report. Key words must be selected so that no security classification is required. Identifiers, such as equipment model designation, trade name, military project code name, geographic location, may be used as key words but will be followed by an indication of technical context. The assignment of links, rules, and weights is optional.